Process Analysis of Elevated Concentrations of Organic Acids at Whiteface Mountain, New York

Christopher Lawrence [1], Mary Barth [2], John Orlando [2], Paul Casson [1], Richard Brandt [1], Dan Kelting [3], Elizabeth Yerger [3], and Sara Lance [1]

[1]Atmospheric Sciences Research Center (ASRC), University at Albany, SUNY ETEC building, 1220 Washington Ave, Albany NY 12226, USA

[2]Atmospheric Chemistry Observations and Modeling Laboratory (ACOM), National Center for Atmospheric Research, Boulder, CO 80301, USA

[3]Paul Smith's College Adirondack Watershed Institute (AWI), P. O. Box 265, Routes 86 and 30, Paul Smiths NY 12970, USA

Correspondence: Christopher E. Lawrence (celawrence@albany.edu)

Abstract. Organic acids represent an important class of compounds in the atmosphere but there ~~are many uncertainties in understanding their formation; in particular, few investigations have been carried out as to their sources~~ is limited research investigating their chemical production, particularly in the Northeast U.S. ~~Associated~~ To improve our understanding of organic acid sources, a modeling analysis was performed for air masses reaching the summit of Whiteface Mountain (WFM), New York where measurements of organic acids in cloud water have been collected. The analysis focuses on a pollution event associated with a heat wave ~~and pollution event~~ that occurred on 1-2 July, 2018 ~~,~~ that exhibited unusually high concentrations of formic (HCOOH), acetic (CH_3COOH), and oxalic (OxAc) acid in cloud water~~were measured at the summit of Whiteface Mountain (WFM) in upstate New York. To investigate the gas~~. Gas phase production of organic acids for this pollution event ~~, this work uses~~ was modeled using a combination of the regional transport model WRF-Chem, which gives information on transport and environmental factors affecting air parcels reaching WFM, and the Lagrangian chemical box model BOXMOX, which allows analysis ~~analysi~~ of chemistry with different chemical mechanisms. Two chemical mechanisms are used in BOXMOX: 1) the Model for Ozone and Related chemical Tracers (MOZART T1), and 2) the Master Chemical Mechanism version 3.3.1 (MCM). The WRF-Chem results show that air parcels sampled during the pollution event at WFM originated in central Missouri, which has strong biogenic emissions of isoprene. Many air parcels were influenced by emissions of nitrogen oxides (NO_x) from the Chicago Metropolitan Area. ~~Ozonolysis~~ The gas-phase oxidation of isoprene and its related oxidation products ~~were the major sources of HCOOH in both mechanisms. CH_3COOH was produced from acetyl peroxy radical (CH_3CO_3) reacting with the hydroperoxy (HO_2) radical, with MCM producing up to 40% more CH_3COOH under conditions of high isoprene and low NO_x compared to MOZART T1. Both mechanisms underpredicted HCOOH and and~~ was the major source of HCOOH and CH_3COOH ~~by an order of magnitude compared to measurements at WFM~~but both mechanisms substantially underproduced both acids compared to observations. A simple gas+aqueous ~~box model was used to determine if cloud water chemistry could have had an appreciable impact~~ mechanism was included to investigate the role of aqueous chemistry on organic acid ~~formation. The addition of aqueous chemistry exacerbated the discrepancies of HCOOH with observations by leading to a net depletion within cloud water. There were large disagreements in the production of glyoxal (a key precursor of OxAc) between the two~~

~~gas-phase mechanisms, with MOZART T1 showing stronger daytime production under high~~ production. Aqueous chemistry did not produce more HCOOH or CH_3COOH, suggesting missing chemical sources of both acids. However this aqueous chemistry was able to explain the elevated concentrations of OxAc. Anthropogenic NO_x ~~conditions, while MCM showed strong nocturnal production via ozonolysis chemistry. The gas + aqueous model exhibited strong production of OxAc within cloud droplets, with glyoxal serving as an important precursor. The substantial differences between chemical mechanisms and between observations and models indicates that further~~ emissions from Chicago had little overall impact on the production of all 3 organic acids. Further studies are required to better constrain gas and aqueous production of low molecular weight organic acids.

1 Introduction

Organic acids are an important class of compounds in the atmosphere that can represent an important fraction of organic aerosol, comprising up to 52 % of the water soluble organic carbon mass. (Sorooshian et al., 2007; Miyazaki et al., 2009; Kawamura and Bikkina, 2016; Kawamura et al., 2017). Organic acids can also contribute a large fraction of the acidity in cloud and rain water, particularly in remote and rural regions (Pye et al., 2020), and may contribute to new particle formation (Zhang et al., 2004, 2017; Kumar et al., 2019). Additionally, there is a growing evidence that organic acids are important in partitioning ammonia (NH_3) into ambient aerosol (Tao and Murphy, 2019; Li et al., 2021) and cloud water (Lawrence et al., 2023). Organic acids are ubiquitously found throughout the atmosphere, measured in locations including the Arctic (Mungall et al., 2018; Feltracco et al., 2021), urban environments, (Souza et al., 1999; Avery et al., 2001), biomass burning smoke plumes (Chaliyakunnel et al., 2016), and forested areas (Fulgham et al., 2019; Eger et al., 2020). Despite their ubiquity and their growing chemical importance in many regions around the world, ~~they~~ organic acids are often not routinely included in studies monitoring the chemical composition of cloud and rain water and are rarely investigated in detail within modeling studies ~~. To address these shortcomings~~in either the gas or aqueous phase. To contribute to the limited body of research, this study investigates the key processes in both the gas and aqueous phases that led to unusually high concentrations of organic acids measured in Whiteface Mountain (WFM) cloud water on July 1st, 2018.

Formic (HCOOH) and acetic (CH_3COOH) acids are typically the most abundant monocarboxylic acids found in the atmosphere (Paulot et al., 2011; Link et al., 2020). Primary sources of HCOOH and CH_3COOH include soil emissions, (Mielnik et al., 2018), biomass burning (Chaliyakunnel et al., 2016) and even certain species of ants (Graedel and Eisner, 1988; Legrand et al., 2012). HCOOH and CH_3COOH are also produced from the atmospheric oxidation of VOCs (Figure 1). It is thought HCOOH and CH_3COOH are largely biogenic in origin but are also known to have important anthropogenic sources regionally including fossil fuel combustion and volatile chemical products. In particular, the oxidation of isoprene and its related oxidation products are considered the most important precursor VOCs. Even though these acids are commonly found in the atmosphere,

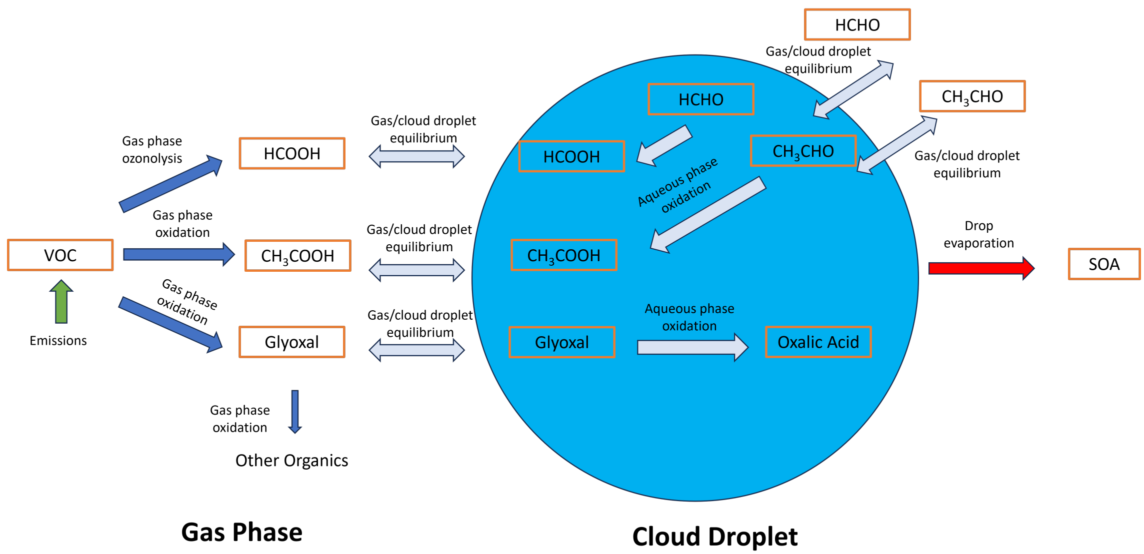

Figure 1. Summary of the major processes controlling organic acid production including emissions of VOCs, gas phase oxidation to form HCOOH and CH_3COOH and the important precursor glyoxal, gas/cloud equilibrium partitioning ,and the aqueous oxidation that either produces or removes organic acids. Important secondary organic aerosol chemistry is ignored to maintain simplicity of the schematic.

they are typically underpredicted by current gas phase mechanisms, especially HCOOH (Millet et al., 2015; Yuan et al., 2015; Chen et al., 2021), with the underlying causes remaining unclear.

More recent work has revealed that cloud droplets may act as an important medium for the formation of organic acids. Volatile but highly water soluble gases like glyoxal can dissolve into cloud droplets, where they subsequently oxidize to form dicarboxylic organic acids such as oxalic acid (OxAc) (Figure 1) that remain within the particle phase after the cloud droplets evaporate ~~(Blando and Turpin, 2000; Crahan et al., 2004; Lim et al., 2005; Warneck, 2005; Ervens et al., 2003; Sorooshian et al., 2006; Ti~~ (Blando and Turpin, 2000; Lim et al., 2005; Warneck, 2005; Ervens et al., 2003; Sorooshian et al., 2006; Carlton et al., 2007; Tan et al., 20 . This process is especially important for the formation of dicarboxylic acids like OxAc as they have no known secondary gas phase sources, while primary emissions cannot explain their atmospheric concentrations (Yao et al., 2004). Despite the prevalence of this chemistry, these processes are often ignored or are oversimplified in chemical transport models.

At the summit of WFM in upstate NY, there is an historic cloud water monitoring program that has been operating since 1994. This program was initially focused on investigating the formation of two acid deposition species, sulfate (SO_4^{2-}) and nitrate (NO_3^-), and was subsequently funded to monitor progress of the Clean Air Act Amendments of the 1990s. In more recent years, as the prevalence of acid deposition has decreased at WFM and throughout the United States, attention has shifted toward the organic fraction of cloud water ~~(?Lawrence et al., 2023)~~(Schwab et al., 2016; Lawrence et al., 2023). Starting in 2018, organic acids were added to the suite of regularly measured chemical species within cloud water which include HCOOH, CH_3COOH, and OxAc.

On July 1-2 2018, collected cloud samples exhibited unusually high concentrations of these organic acids with the underlying causes remaining unexplored. As the influence from SO_4^{2-} and NO_3^- in cloud water has decreased at WFM, at the same time that the influence from organic carbon has increased (Lawrence et al., 2023), the importance of organic acid contributions to the chemical system has grown, requiring a better characterization of the their underlying chemistry. Chemical transport models can be used to study the production of organic acids. However, it is challenging to investigate the major chemistry involved in their production upwind of a given location. Chemical box modeling can be used for a detailed look at the chemistry of organic acid production but the initial conditions and emissions of many chemical species, particularly VOCs, are limited both spatially and temporally. To overcome these limitations, a combination of chemical transport modeling and Lagrangian chemical box modeling can be used be to investigate organic acid production.

The current study used a combination of the chemical transport model Weather Research and Forecasting Model with Chemistry (WRF-Chem; Grell et al. (2005); Fast et al. (2006)) and the gas phase chemical box model BOXMOX (Knote et al., 2015) to evaluate the gas-phase chemistry affecting the high concentrations of organic acids at WFM during this pollution event. WRF-Chem simulations were performed for the heat wave and pollution event to provide the necessary meteorological and chemical input data to conduct Lagrangian chemical box modeling. BOXMOX was subsequently used for a detailed assessment of the gas-phase chemistry involved in organic acid production. Gas phase box modeling results are compared to cloud water measurements made at WFM. Additionally, a simple gas + aqueous box model was employed to determine if cloud chemistry contributed to overall organic acid concentrations. Finally, the impacts of anthropogenic emissions on organic acid production will be discussed.

2 Description of the Pollution Event

The July 1-2, 2018 pollution event was chosen as case a study to investigate the chemical production of organic acids. This event impacted much of the northeast United States, including WFM, coinciding with a regional heat wave with temperatures reaching 35° C (Figure S1) in several locations. Many locations, particularly the New York City Metropolitan area, saw O_3 mixing ratios exceeding National Ambient Air Quality Standards, with mixing ratios reaching over 100 ppbv. (Tian et al., 2020; Tran et al., 2023).

2.1 WFM Observations

At WFM, concentrations of several chemical species including organic acids in both cloud water and in the gas phase were considerably greater than normal during this event. Information about cloud water collection protocols at WFM can be found in Lawrence et al. (2023). Briefly, an automated Mohnen omni-directional cloud water collector is used to collect warm cloud water (i.e. $>$ >0°C) form from non-precipitating clouds between the months of June and September. Samples were collected in a refrigerated accumulator that dumps into a refrigerated sample bottle every 12 hours. Samples were then analyzed for sulfate (SO_4^{2-}), nitrate (NO_3^-), ammonium (NH_4^+), calcium, (Ca^{2+}), magnesium (Mg^{2+}), potassium (K^+), sodium (Na^+), chloride (Cl^-), pH, conductivity, water soluble organic carbon (WSOC), and organic acids, including HCOOH, CH_3COOH, and OxAc.

Organic acids were measured by the Adirondack Watershed Institute using a Lachat QC 8500 Ion Chromatograph, along with SO_4^{2-} and Cl^-. A manuscript focusing on the organic acid measurement methods and observations will be submitted separately. The current work focuses on three of the measured organic acids, HCOOH, CH_3COOH and OxAc, as these are the three most common organic acids found in cloud water at WFM and other locations (Herckes et al., 2013). While the exact detection limits of the organic acid analysis is currently being determined, a conservative estimate of 50 μg L^{-1} for all 3 organic acids is used, based on the lowest concentration calibration standard. It is worth noting that the concentrations of the 3 organic acids investigated in this study are well above this conservative detection limit, with concentrations of 113, 111, and 23 times greater than the lowest concentration standard used in the calibrations respectively. Trace gases are measured continuously year-round, with chemical species including ozone (O_3), oxides of nitrogen (NO, NO_2 and NO_y), and sulfur dioxide (SO_2). More information about the gas phase dataset can be found in (Brandt et al., 2016).

The pollution event consisted of some of the highest concentrations of the season for SO_4^{2-}, NH_4^+, WSOC, HCOOH, CH_3COOH, and OxAc. (Figure 2), with individual samples of HCOOH and CH_3COOH exhibiting concentrations greater than 100 μeq L^{-1} and contributing to approximately 30% of measured anions. Additionally, O_3 and NO_y mixing ratios were above the 90th percentile of mixing ratios for this event, as compared to the rest of the 2018 summer season (June through September), coinciding with the highest temperatures of the cloud collection season (Figure S2). The relatively high mixing ratios of these trace gases may indicate significant anthropogenic influence. The cloud event focused on two cloud samples collected between 7/1/2018 0:00 UTC and 7/1/2018 15:00 UTC, with cloud liquid water content (LWC) values reaching up to 1.25 g m^{-3} (Figure S4). The July 1^{st} event was chosen for the modeling study as the duration of this cloud event was substantially longer than the event on July 2^{nd} , making it better suited for modeling.

2.2 Determining Total Organic Acid Mixing Ratios from Cloud Water Observations

Currently at WFM, organic acids are measured only within cloud water. However, substantial concentrations of low molecular weight organic acids have been previously shown to be in the gas phase (Khwaja, 1995). Gas phase and total mixing ratios of organic acids can be estimated, assuming the organic acid is in equilibrium with the atmosphere, as a function of the acid's Henry's Law constant, cloud LWC, temperature, pressure, and pH of the cloud droplets using the following equation:

$$\mathrm{OrgAcid_{tot}} = 10^{12}(*\frac{\mathrm{Q_{LWC}(RT)OrgAcid_{aq}}}{\mathrm{P}} + \frac{\mathrm{OrgAcid_{aq}}}{\mathrm{K_{Heff}P_{atm}}}) \quad (1)$$

where $\mathrm{OrgAcid_{tot}}$ is the calculated sum of gas phase and aqueous phase organic acid mixing ratios in pptv, 10^{12} is a conversion factor to convert the mixing ratio to pptv, Q_{LWC} is the cloud LWC in L m^{-3}, R is the universal gas constant (8.314 m^3 Pa $K^{-1}mol^{-1}$), T is the ambient temperature in K, P is the ambient pressure in Pa, $\mathrm{OrgAcid_{aq}}$ is the concentration of the specific organic acid measured in the cloud water in mol L^{-1}, P_{atm} is the ambient atmospheric pressure in atm, $\mathrm{K_{Heff}}$ is the temperature and pH dependent effective Henry's law constant for the given organic acid in mol atm^{-1}. The pH dependency of $\mathrm{K_{Heff}}$ for monocarboxylic acids can be calculated by:

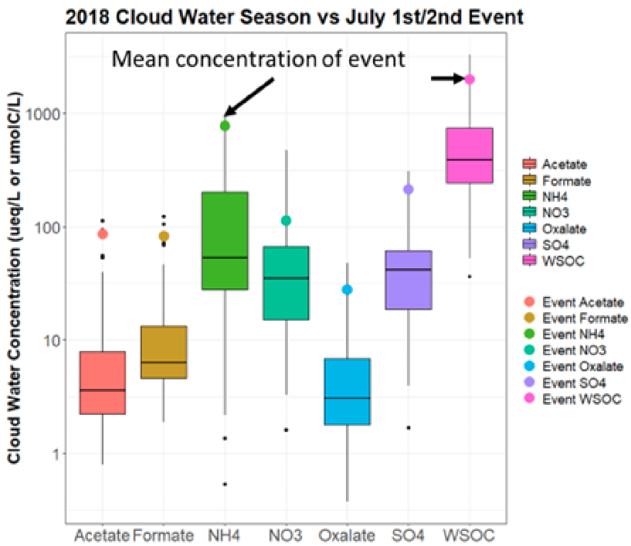

Figure 2. Cloud water concentrations of Acetate (CH_3COOH), formate ($HCOOH$), NH_4^+, NO_3^-, oxalate (OxAc), SO_4^{2-}, and WSOC from the 2018 of June-September cloud water season. WSOC is reported in units of μmol C L^{-1}, whereas all other analytes are reported in units of μeq L $^{-1}$. The 25th, 50th, 75th percentiles are marked by the colored boxes, the vertical lines represent the 1.5* the inter-quartile range, and the black dots represent values outside the vertical lines.

$$K_{Heff} = K_H(1 + \frac{K_a}{[H^+]}) \tag{2}$$

while for dicarboxylic acids, K_{Heff} can be calculated by:

$$K_{Heff} = K_H(1 + \frac{Ka_1}{[H^+]} + \frac{Ka_1 Ka_2}{[H^+]^2}) \tag{3}$$

where K_H is the standard Henry's law constant of the organic acid, K_a is the acid dissociation constant for monocarboxylic acids, Ka_1 and Ka_2 are the first and second dissociation constants for dicarboxylic acids and $[H^+]$ is the acidity of the cloud droplets. The temperature dependence of the Henry's Law constant is :

$$K_{Heff} = K_H * \exp(\frac{\Delta H_s}{R} * (\frac{1}{T_2} - \frac{1}{T_1})) \tag{4}$$

where T_2 is the ambient temperature, T_1 is the reference temperature of 298.15 K, and ΔH_s is enthalpy of dissolution described in Sander (2023) . The values used for the above calculations can be found in Table S1. K_H values of $HCOOH$, CH_3COOH and OxAc are taken from Sander (2023), while K_a values were taken from Seinfeld and Pandis (2016). The associated pH values of the two cloud samples used in this study are 4.50 and 4.56, while the temperatures are 292.17 K and 292.12 K respectively.

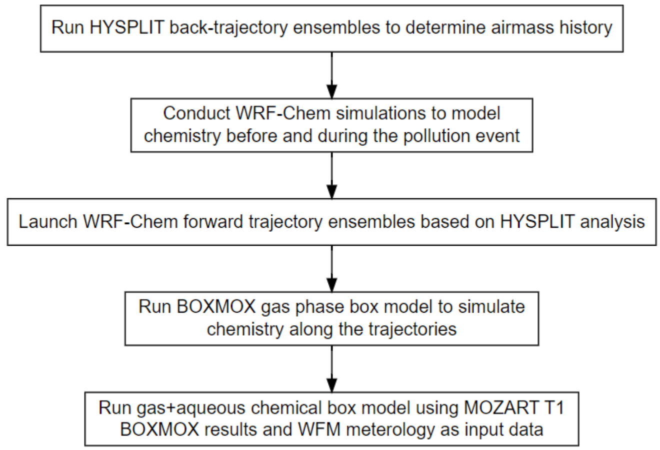

Figure 3. Procedure for the modeling analysis organic acids.

3 Modeling Setup

This work uses a combination of modeling techniques, including ensembles of HYbrid Single-Particle Lagrangian Integrated Trajectory (HYSPLIT) back-trajectories (Stein et al., 2015), the WRF-Chem chemical transport model, gas-phase box modeling, and box modeling of gas and aqueous chemistry. This methodology is used to allow for more detailed investigation of the underlying chemistry impacting organic acid formation. It is challenging to investigate chemical processing of an air mass upwind of a location in detail using chemical transport models alone. A Lagrangian approach coupled with a chemical box model allows for the detailed investigation of the underlying chemistry involved in the production of organic acids. Figure 3 summarizes the step by step procedure for this modeling process.

3.1 HYSPLIT Back Trajectory Analysis

Three-day ensemble back trajectory analysis was conducted to determine the source location of the pollution event using the (HYSPLIT) model (Stein et al., 2015). The receptor site for the trajectories is the summit of WFM, 44.37° N, 73.9° W, 1500 m above sea level. The meteorological data used for these calculations was the North American Mesoscale (NAM) 12kmx12km dataset (more information on the meteorology data can found at https://www.ready.noaa.gov/archives.php). The trajectories consistently flew near the surface in central Missouri near Jefferson City approximately 2 days prior to the pollution event at WFM (Figure 4). This location was therefore chosen to launch the WRF-Chem forward trajectories.

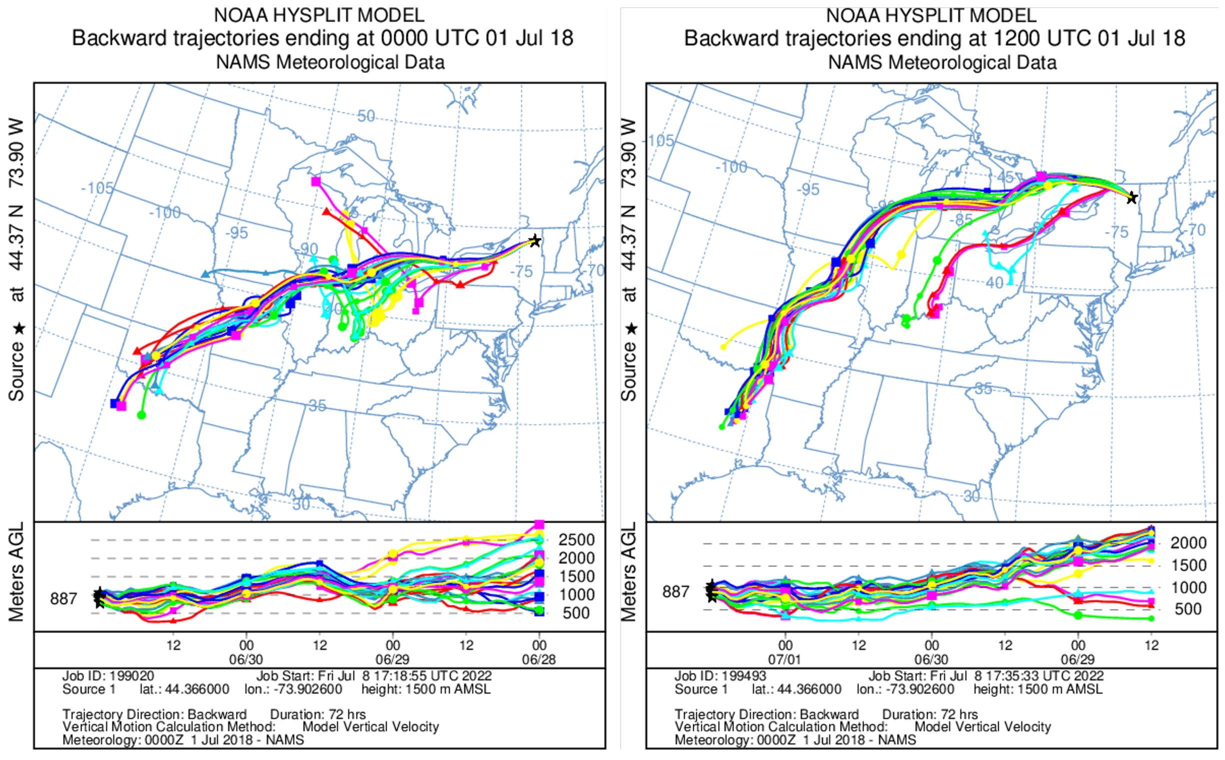

Figure 4. HYSPLIT back-trajectory ensembles ending at the summit of WFM (1500m) on July 1st, 2018 at 0:00 UTC and 12:00 UTC. Trajectory ensembles typically flew over Jefferson MO.

3.2 WRF-Chem

3.2.1 Model Run Description

The chemical transport model used for these simulations was the Weather Research and Forecasting Model with Chemistry (WRF-Chem) v4.0.3 (Grell et al., 2005; Fast et al., 2006). Multiphase chemistry including gas, aerosol, clouds, and rain were included within the simulation. A five-day simulation was performed from 6/27/2018 0:00 UTC to 7/2/2018 12:00 UTC with a 12kmx12km horizontal grid resolution and 43 vertical layers from the surface to 50 hPa. A detailed description of the WRF-Chem simulation parameters and a map of the WRF-Chem domain can be found in section S3 and Figure S3 of the supplemental material.

3.2.2 WRF-Chem ~~Results and~~ Evaluation

O_3 and PM ~~$_{2.5}$~~ 2.5 data collected by the EPA's Air Quality System (AQS) monitoring program (EPA, 2024) were used to evaluate the capabilities of WRF-Chem to represent the pollution event. ~~There is reasonable agreement of surface O_3 and $PM_{2.5}$ in the simulations compared to observations collected before and during the pollution event in the Northeast U.S.~~

(Figure 5). The airmass associated with this pollution event was characterized by a combination of high temperatures over the Great Plains region that moved eastward towards the Great Lakes region before reaching the Northeast, under the influence of a large high pressure system. WRF-Chem properly captured the warm temperatures that moved across the Midwest into the Northeast (Figure S5). These meteorological conditions contributed to O_3 mixing ratios in excess 70 ppbv large over large portions of the Midwest on June 29th, 20:00 UTC before spreading to the Northeast US including WFM on July 1st 20:00 UTC. Additionally, PM 2.5 levels rose to levels >15 μg m^{-3} throughout much of the Eastern U.S. on July 1st, 2018, including WFM (Figure 5). There was potential evidence for an influence from wildfire activity from the Southeast U.S. according to the WRF-Chem simulations, but it was unclear if emissions from these fires contributed significantly to the pollution event. To determine potential fire impact, a WRF-Chem simulation that did not include any biomass burning emissions was run for the same time interval as the original simulations. Comparisons of these simulations found virtually no contribution of biomass burning emissions to $PM_{2.5}$ mass concentrations, O_3 mixing ratios, or trace gases important in the formation of organic acids (Figure S6), indicating this pollution event was primarily driven by biogenic and/or anthropogenic emissions.

Modeled O_3 exhibited a strong positive linear correlation (r >0.8) with observations across the model domain, but consistently exhibited a mean bias error (MBE) of 10+ ppbv on June 29th and July 1st (Figures S7 and S8). This high bias in O_3 has been reported in other recent works (Travis et al., 2016; Schwantes et al., 2020; Place et al., 2023) which may be due to overestimated NO_x emissions and/or improper representation of gas-phase organic chemistry. Note that the 2017 EPA NEI used in this study is appropriate for a typical summer day and will likely not represent the actual emissions of the heatwave period caused by the stagnation event. Heatwaves can increase demand on the grid (Maia-Silva et al., 2020; Stone et al., 2023) and therefore increase NO_x emissions due to greater combustion of fossil fuels from power generation (Chen et al., 2015), which are not represented by the 2017 NEI. Given the potential low bias in modeled NO_x emissions, the high bias in modeled O_3 is even more perplexing, highlighting the complex chemistry involved in O_3 production.

Importantly, the modeled MBE for O_3 is <10 ppbv for central Missouri on June 29th, and Western New York on July 1st, locations that were upwind of WFM according to the HYSPLIT trajectories. This indicates that O_3 chemistry was well represented in the airmass that traveled to WFM. $PM_{2.5}$ model predictions performed worse compared to O_3 with many linear correlation values exhibiting null or negative values and MBE exceeding 10 μg m^{-3}. Similar to O_3, model MBE was <10 μg m^{-3} for Missouri and much of Chicago on June 29th and Western New York on July 1st.

Three air quality monitoring sites in New York measuring O_3, $PM_{2.5}$, and 2 meter temperature were chosen for time-series evaluations of WRF-Chem, including Pinnacle State Park (PSP) in the Southern Tier of New York, Queens College in New York City, and measurements at both the summit and the the old ski lodge below the summit of WFM (Figure S7S9). More information about the data collected at these sites can be found in Brandt et al. (2016) and Ninneman et al. (2020). There is strong agreement between model and observations for both temperature and O, while Pearson correlation values and MBE statistics can be found in Figure S9. WFM tends to show the lowest linear correlation with observations. This is likely due to WRF-Chem underestimating the elevation of WFM (1483m) by over 700m, and therefore not properly accounting for the topography in the region (Figure S10). By using a 12 km x 12 km horizontal grid mesh in WRF-Chem, the topography is not well represented resulting in the modeled WFM summit to be underestimated by approximately 700 m and affecting

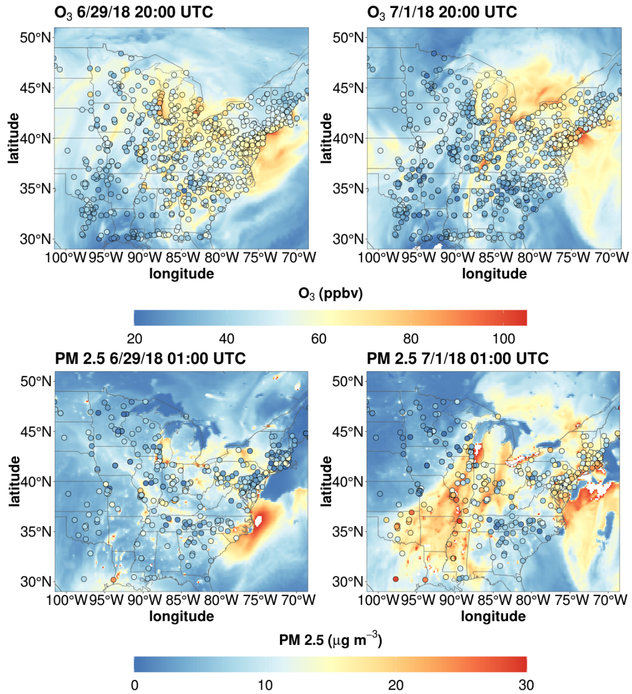

Figure 5. WRF-Chem Results for ~~: a) Ozone~~ ozone and ~~b)~~ $PM_{2.5}$ before and during the pollution event that impacted the northeast U.S. Points represent monitoring station observations from the U.S. EPA's AQS monitoring program

the capabilities of WRF-Chem to represent mountain-valley winds and timing of when the summit is above and within the PBL (Giovannini et al., 2020) . PSP shows the lowest MBE values with high correlation coefficients (r >0.7) for O_3 ~~at PSP and Queens College after allowing for 24 hours of model spin up time. However, there is fairly substantial disagreement at WFM for temperature and~~ and 2m temperature. Finally, Queens college saw the strongest correlation coefficients for O_3 ~~. The complex geography of the Adirondack Mountains are likely not properly captured with a 12kmx12 km horizontal grid resolution, which may cause local meteorological conditions to be modeled improperly, particularly as it relates to the planetary boundary layer. However, WRF-Chem demonstrates skill in both rural and urban settings with simpler geography, indicating that the simulations are producing realistic conditions of traditionally modeled compounds like O~~and 2m temperature (r >0.85), but exhibited large positive biases for O_3 ~~. $PM_{2.5}$ shows reasonable agreement between model and observations for WFM and PSP, but is greatly overpredicted at Queens College~~and $PM_{2.5}$. The causes behind ~~this overprediction~~ these overpredictions remain unclear but are beyond the scope of this work.

3.2.3 Forward Ensemble Trajectory Analysis

A feature in WRF-Chem is to monitor air masses through forward trajectories. With an input file, trajectories can be launched at specified latitude-longitude-height locations and times. The trajectory code uses resolved winds (u, v, w) to determine the location of the air mass at each time step. Several variables can be monitored along the trajectory including prognostic and diagnostic information (https://www2.acom.ucar.edu/sites/default/files/documents/Trajectory.desc_.pdf). During the WRF-Chem simulation, 10 sets of 75 forward trajectories were launched near Jefferson City, Missouri at 38.5° N and 92.5° W. This location was chosen based on the HYSPLIT back trajectory analysis. The starting latitude and longitude of the trajectories was perturbed by +/- 0.1° and +/- 0.2° and were launched at 3 starting heights of 750m , 1000m and 1250m every 2 hours starting at 6/28/2018 22:00 UTC and ending at 6/29/2018 16:00 UTC. To limit analysis to trajectories that influenced WFM, only trajectories that flew within 1° latitude and longitude and below 3000m AGL were considered for chemical box modeling. Of the 750 trajectories launched, 556 trajectories (74.1%) reached WFM.

3.2.4 Chemical Box Modeling

The chemical box model, BOXMOX, was used to simulate the gas phase chemistry along the trajectory pathways. BOXMOX uses a Kinetic PreProcessor (KPP) with a Rosenbrock ODE solver (Knote et al., 2015). Necessary box model input parameters were obtained from output data from the WRF-Chem forward trajectories, providing information for initial conditions, emissions (biogenic, anthropogenic, and biomass burning), background conditions, ~~gas phase~~ photolysis rate constants, and environmental conditions (temperature, pressure, planetary boundary layer height). Initial conditions are determined by using the mixing ratios at time 0 of the launch locations of the given trajectory. Photolysis rates were provided at a 15 minute time resolution. while emissions, environmental conditions, and background conditions were provided at a 1 hour time resolution. Emissions were assumed to be zero if the trajectory height was above the top of the boundary layer. In order to account for entrainment of background air into the air parcel, a first order mixing rate constant was set to 1.17x10^{-5} s^{-1}, associated with a dilution time of approximately 24 hours, consistent with values used in other works (Wolfe et al., 2016; Decker et al., 2019). Sensitivity analysis of this dilution constant in Section S7 reveals that while there were noticeable impacts on organic acid production, the conclusions of this work were not impacted (Figure ~~S8~~S11), as will be discussed further in Section 4. Background air is determined by a 60x60km WRF-Chem average mixing ratios of the chemical species of interest at the height of the trajectory.

Two gas phase mechanisms were used for the BOXMOX simulations; the Model for Ozone and Related chemical Tracers version (MOZART) T1 and the Master Chemical Mechanism (MCM) version 3.3.1. Two mechanisms were chosen to determine if a simpler mechanism is sufficient in simulating organic acid chemistry that is more explicitly represented in the more complex mechanism of MCMv 3.3.1. MOZART T1 contains 151 chemical species and 352 gas phase reactions, as described in Emmons et al. (2020). MCM is a highly detailed chemical mechanism containing 142 emitted non-methane VOC species and nearly 17,000 reactions (Jenkin et al., 2015). The MOZART T1 mechanism simplifies the chemistry of larger VOC species by grouping their chemistry into categories of lumped species. These VOCs include BIGALK (alkane species with more than 3 carbons), BIGENE (alkenes with more than 3 carbons) and XYLENES (all XYLENE species and alkyl benzene species but not TOLUENE or BENZENE). However, the individual VOCs that make up these lumped species are directly represented in MCMv 3.3.1 and need to be translated in to realistic atmospheric mixing ratios. Initially, this was done by using whole air sampler VOC data collected by UC Irvine during the KORUS-AQ field campaign to determine what the average fraction of the lumped species was represented by an individual species. However, a sensitivity study using MCMv 3.3.1 was conducted by setting initial conditions and emissions of the lumped species to 0 to determine if they have a significant role in organic acid production (Figure S9S12). The results showed that there were virtually no differences in organic acid mixing ratios when removing the lumped species from the simulations and therefore the contributions of their chemistry are assumed to be negligible.

3.2.5 Gas + Aqueous Chemical Box Model

In addition to the gas phase box modeling, a simplified gas + aqueous box model was introduced to study the effects of aqueous chemistry effects on organic acid concentrations for the analyzed pollution event. Detailed information on the aqueous box model can be found in Li et al. (2017) and Barth et al. (2021). Briefly, the gas + aqueous box model contains a simplified gas phase mechanism with 64 reactants and 168 reactions. Gas-aqueous phase partitioning of low solubility or slow reacting species is controlled by their Henry's Law coefficients while high solubility species (such as HNO_3) or fast reacting species (OH, HO_2, NO_3 radicals) are controlled by the resistance model developed by Schwartz (1986). The aqueous mechanism contains 45 reactions including conversion of sulfur dioxide (SO_2) to SO_4^{2-} via hydrogen peroxide (H_2O_2) and O_3, and the oxidation of C1-C3 carbonyls and organic acids via OH the radical.

A limitation of these simulations is that the forward trajectories produced by WRF-Chem contained no cloud LWC, preventing the inclusion of cloud water chemistry along the trajectories, despite the observed cloud event at WFM. Therefore, a set of stationary aqueous box model simulations were run at the summit of WFM. Hourly meteorological measurements at the summit of WFM (including LWC, temperature, and sea-level pressure) were used to constrain these aqueous simulations. A complication of stationary box models is the need to account for advection of air upwind of a given location. To minimize the potential influence of changing air masses, model runs were limited to 3 hours, with 30 minutes of gas phase only chemistry at the beginning of each simulation, assuming negligible advection and emissions in this timeframe. Three-hour simulations were run each hour from 6/30/2018 12:00 to 7/1/2018 13:00 EST including periods before, during, and after the polluted cloud event at WFM. Initial conditions of gas phase species were provided from hourly averaged mixing ratios from the MOZART T1 BOXMOX results within 1° latitude and longitude of WFM. The authors emphasize that while these aqueous modeling methods are highly simplified, the purpose of the aqueous modeling is to determine whether clouds were likely to have had an appreciable impact on organic acid mixing ratios for this pollution event, rather than trying to precisely quantify the impact of cloud chemical processing on organic acid concentrations.

4 Gas Phase Box Model Results

4.1 Forward Trajectories

There is very little temporal variability in the WRF-Chem trajectory ensembles during the pollution event based on the median trajectory positions for each launch time, consistent with the HYSPLIT back trajectory results (Figure 6a). Median trajectories

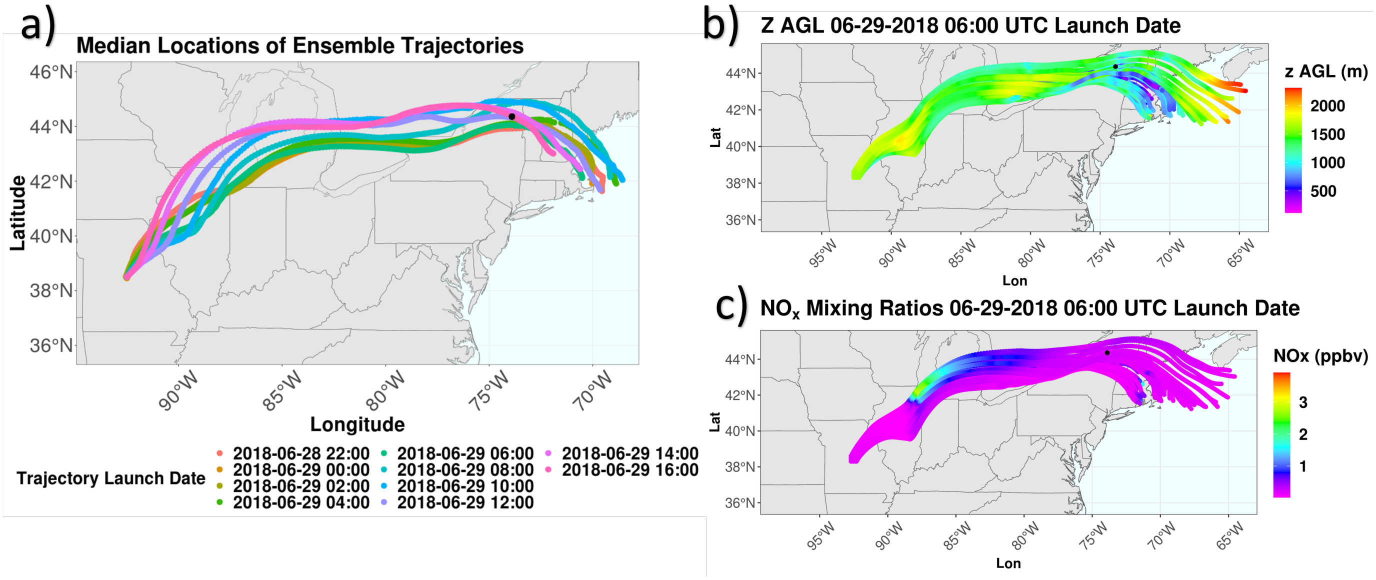

Figure 6. a) Median locations of forward trajectory ensembles launched in WRF-Chem, colored by launch date. Forward trajectory ensembles for trajectories launched on 06/29/2018 at 6:00 UTC colored by b) trajectory height above ground level (m), and c) NO_x mixing ratios

rather than mean values are used as median values tend to be less sensitive to outliers than mean values (Wilcox, 2012). The ensemble trajectories indicate that many trajectories are within the boundary layer and are influenced by NO_x emissions from the Chicago Metropolitan Area (Figure 6c). The full set of trajectory ensembles can be found in Figure ~~S10~~S13. The trajectories largely travel eastward, with little horizontal variation between the trajectories at each launch date, indicating minimal uncertainty in the forward trajectory analysis. Many trajectories experience significant increases of NO_x, up to 4 ppbv, as the airmasses advect over the Chicago Metropolitan area, the likely source of anthropogenic influence on the airmass impacting WFM. Some trajectories (particularly those launched from 2018-06-29 10:00 UTC and 12:00 UTC) are also influenced by emissions from Toronto, ON.

Time series of O_3 and NO_x for each of the 10 launch dates reveal good model agreement between MOZART T1 and MCMv 3.3.1 results, indicating that the simpler chemistry within MOZART T1 is sufficient in capturing O_3 mixing ratios, which vary only slightly (45-60 ppbv) but typically increase as the simulations progress (Figure ~~S11~~S14). Many of the trajectories launched from Missouri show enhanced mixing ratios of isoprene, with median mixing ratios of up to 5 ppbv (Figure ~~S12~~S15). This is consistent with previous work within the Ozark region of Missouri (Carlton and Baker, 2011; Schwantes et al., 2020), and is exhibited by the WRF-Chem simulations (Figure ~~S13)~~S16).

4.2 Formic and Acetic Acid

4.2.1 HCOOH Production

There is significant net production of HCOOH by both chemical mechanisms (MOZART T1 and MCM) for all of the trajectory launch dates, particularly for trajectories launched on 6/28 22:00 UTC, 6/29 00:00 UTC and 6/29 10:00 UTC, peaking at mixing ratios of 300 pptv (Figure 7). For all simulations, both mechanisms are in near agreement, with strong production for many sets of trajectories being confined to early in the simulations, before mixing ratios become more controlled by background conditions as emitted VOC precursors are exhausted. HCOOH for both mechanisms is almost entirely produced by the ozonoylsis of isoprene and isoprene oxidation products, mainly methyl vinyl ketone (MVK) and methacrolein (MACR) (Figure ~~S14~~S17). At low mixing ratios of isoprene (~~<~~ $<$500 pptv), ethene (C_2H_4) becomes the dominant source of HCOOH in MOZART T1, but in these instances, dilution is the major controlling factor. It is worth noting that background mixing ratios of HCOOH are about 5-6 times lower than the peak mixing ratios within the box model simulations, ~~leading to significant reductions in~~ decreasing HCOOH mixing ratios to 100-150 pptv as background air is entrained into the air parcel. The low HCOOH mixing ratios in the background data files are caused by the ozonolysis of isoprene, MVK, and MACR not producing HCOOH within WRF-Chem's MOZART-MOSAIC chemistry mechanism. Using the more comprehensive gas phase chemistry in MOZCART mechanism within WRF-Chem (i.e. MOZART T1 + GOCART aerosol scheme) increases mixing ratios of HCOOH up to 150 pptv (Figure ~~S15~~S18). The MOZART-MOSAIC chemistry module was used to simulate aerosol and cloud chemistry for this study to have a more complete aerosol and cloud chemistry representation that the WRF-Chem T1 chemistry option does not include. Since the background files are extracted from WRF-Chem using the MOZART-MOSAIC, this contributes to a low bias of HCOOH within the box model simulations compared to using the MOZCART mechanism, as discussed in Section 4.2.3.

4.2.2 CH_3COOH Production

The mixing ratios of CH_3COOH reach values ~~>~~ $>$1500 pptv, up to 5 times greater than those of HCOOH (Figure 8). MCM produces more CH_3COOH than MOZART T1 by up to 500 pptv, with the largest differences occurring within the first few sets of trajectories, i.e. trajectories launched on 6/28 22:00 UTC, 6/29 0:00 UTC and 6/29 2:00 UTC. However, the disagreement between the two chemical mechanisms largely disappears in the later set of trajectories, particularly for the ensembles influenced by higher NO_x mixing ratios (specifically ensembles 6/29 4:00-10:00 UTC) . The major production pathway (greater than 90%) for CH_3COOH is the reaction of the acetyl peroxy radical (CH_3CO_3) + the hydroperoxy radical (HO_2) or organic peroxy radicals (RO_2). For low NO_x environments, these peroxy radicals can out-compete reactions with NO, ~~leading to significant~~ increasing the prevalence of this reaction pathway and increasing CH_3COOH production (Figure ~~S16~~S19). There are subtle differences in the chemistry between the two mechanisms that contribute to the overall greater production of CH_3COOH in MCM. During the first 20 hours of all sets of trajectories, mixing ratios of CH_3CO_3 were approximately the same between the two mechanisms (Figure ~~S17~~S20). However, there are important differences in the reactivity of CH_3CO_3 within these simulations, particularly as it relates to RO_2 radicals. While the overall reactivity of CH_3CO_3 with RO_2 radicals is greater in MOZART

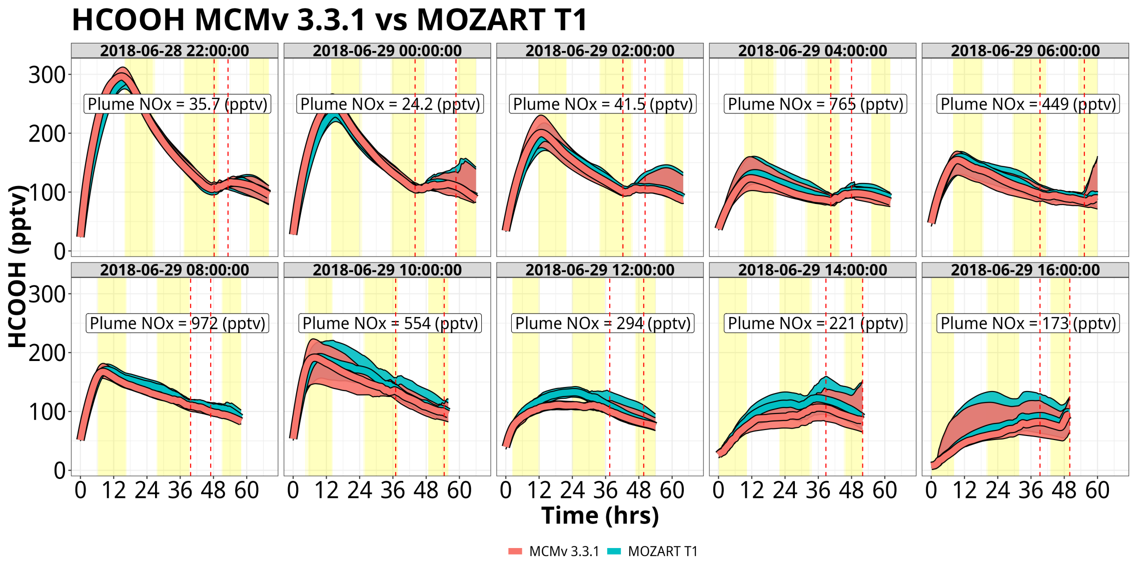

Figure 7. Simulation time series of HCOOH mixing ratios for Mozart T1 (blue) and MCM (red) for the WRF-Chem forward trajectory ensembles, separated by launch time. Red and blue lines represent the median value for the ensemble with the shading represents the interquartile range. Yellow shading represents daylight hours. Vertical dashed lines represent the range of times that the trajectories approach WFM. ~~Plum~~ Plume NO_x represents the median NO_x mixing ratios when the trajectories are above the Chicago Metropolitan Area

T1 (as shown in Figure ~~S18~~S21), a larger proportion of reactions from RO_2 radicals in MCM result in CH_3COOH formation. MCM treats the rate constant and the yield of CH_3COOH from CH_3CO_3 + RO_2 as the methyl peroxy radical (CH_3O_2), while MOZART T1 has only two RO_2 species, CH_3O_2 and MCO_3, that contribute ~~significantly~~ notably to CH_3COOH production. Beyond 20 hours, CH_3CO_3 mixing ratios are up to 2 pptv greater in MCM. This is due to ~~stronger production of methylglyoxal~~ 2x greater methylglyoxal production within MCM vs MOZART T1, an important precursor for CH_3CO_3 from both photolysis and OH (Figure ~~S19~~S22). Disagreements in the rate coefficient for the reaction of OH with peracetic acid also contribute to these discrepancies. Peracetic acid (CH_3CO_3H) is not a direct source of CH_3CO_3 but rather serves as a chemical reservoir. The CH_3CO_3H + OH rate constant is 3.7x greater in MCM compared to MOZART T1, forcing more CH_3CO_3H to shift back to CH_3CO_3 and hence more CH_3COOH. There is evidence that this reaction's rate constant is even slower than what is used in either model, indicating that CH_3CO_3H is in reality even more of a permanent sink for CH_3CO_3, and thus that both mechanisms may overestimate CH_3COOH from this pathway (Berasategui et al., 2020).

4.2.3 Comparison of gas phase chemistry to cloud water observations

In this section we validate the performance of the gas phase chemical box model by comparing the box model results within 1° latitude and longitude of WFM to the derived gas + aqueous phase organic acids (Figure 9). It is assumed that HCOOH and CH_3COOH measured in the cloud water were produced entirely in the gas phase and partitioned into cloud droplets rather

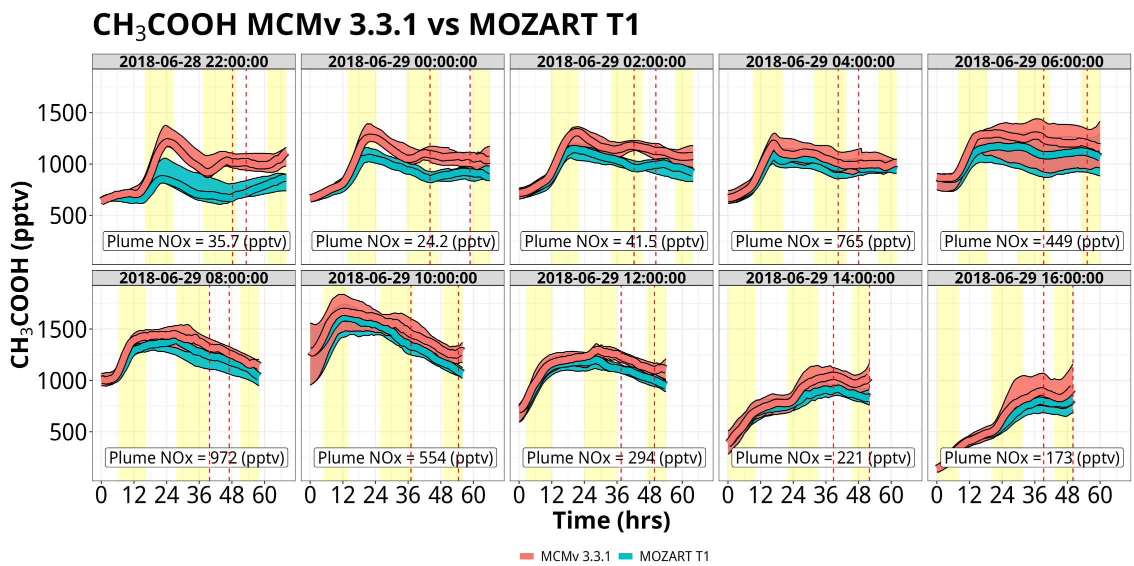

Figure 8. Same as Figure 7 but for CH_3COOH. ~~Plum~~ Plume NO_x represents the median NO_x mixing ratios when the trajectories are above the Chicago Metropolitan Area

than being produced in the aqueous phase, already existing within the aerosol that the cloud droplets activated on, or being directly emitted. It is also important to note that bulk cloud water may deviate from Henry's Law, even if individual cloud droplets may be in equilibrium with the atmosphere. This can be due to differences in pH of individual cloud droplets, mass transfer limitations (especially for highly soluble or reactive species), and changes in equilibrium due to competing reactions. (Pandis and Seinfeld, 1991; Winiwarter et al., 1994; Wang et al., 2020). Despite these uncertainties, comparing the BOXMOX results with observations can indicate if the current chemistry represented in the mechanisms can properly model organic acids in the airmasses arriving at WFM. Average HCOOH mixing ratios increased from 100 pptv to 200 pptv over the course of the simulations, using both mechanisms, while CH_3COOH mixing ratios largely remained constant at approximately 1000 pptv. In spite of the substantial disagreements in gas phase production between the two mechanisms, MCM exhibited only 100-200 pptv more CH_3COOH than MOZART T1 when it arrived at WFM.

The gas-phase box modeling with both MOZART T1 and MCM substantially underestimated both HCOOH and CH_3COOH measured in cloud water by approximately an order of magnitude, implying a ~~significant~~ large missing source of organic acids, which may be from gas, particle, or aqueous phases. As mentioned in Section 4.2.1, there is a low bias in the background conditions from the WRF-Chem simulations due to missing ozonolysis reactions of isoprene, MACR, and MVK. However, even the inclusions of the chemistry in the WRF-Chem simulations cannot explain the order of magnitude underestimation of HCOOH in the BOXMOX results. These results are consistent with other modeling work investigating organic acids, as gas phase box models typically underestimate HCOOH and CH_3COOH production, implying that gas phase chemistry alone is not sufficient to properly model these organic acids (Paulot et al., 2011; Millet et al., 2015; Jones et al., 2017). However, it

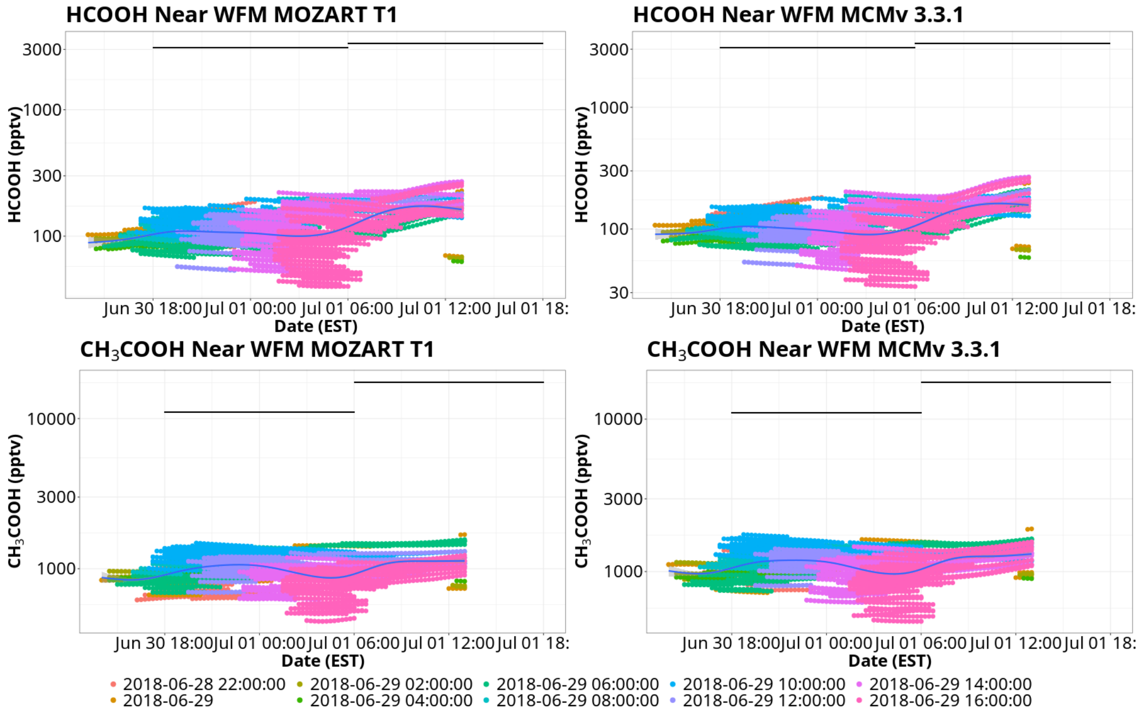

Figure 9. Comparisons of model and observational mixing ratios of HCOOH and CH_3COOH for MOZART T1 and MCM. Points represent modeled mixing ratios from the trajectory ensembles within 1° of WFM, colored by trajectory launch date. Black lines represent the total (gas + aqueous) mixing ratio estimates derived from 12 hour bulk cloud water samples collected at the summit of WFM. The blue line represents a trend line of the BOXMOX results fitted using a generalized additive model

remains unclear the particular reasons for these underestimates. Work by Link et al. (2021) found that ecosystems dominated by isoprene produced greater mixing ratios of organic acids than monoterpene dominated ecosystems, implying that isoprene chemistry not represented in models might be a missing source of HCOOH and CH_3COOH. There is also emerging evidence that cloud droplets may play a unique role in the formation of HCOOH that is not being accounted for in these gas phase simulations. For example, formaldehyde (HCHO) dissolves into cloud droplets, hydrolyzing to form a methanediol, which then partitions back to the gas phase and oxidizes to form HCOOH (Franco et al., 2021). A similar process with other larger aldehydes may be possible, potentially acting as additional sources of larger organic acids.

4.3 Comparison of gas + aqueous chemistry to cloud water observations

Cloud chemistry can ~~have profound impacts~~ alter on organic acid concentrations distinct from gas phase chemistry alone. This section examines the impacts of aqueous chemistry by investigating both total mixing ratios ~~(left)~~ and aqueous concentrations ~~(right)~~ of HCOOH and CH_3COOH using mixing ratios near WFM to initialize the model (Figure 10). The total mixing ratios are useful to show the overall change in organic acid concentrations resulting from chemistry in both phases while the aqueous phase concentrations can be used to directly compare to cloud water measurements. Despite large concentrations of CH_3COOH in the aqueous phase, there is very little change in total mixing ratios of CH_3COOH mixing ratios change by less than 1% throughout these simulations, indicating a limited role of chemistry (within the gas or aqueous phase) on the overall CH_3COOH produced within these gas+aqueous simulations. However, HCOOH is almost completely depleted within the aqueous phase, driven largely by the ionic $HCOO^-$ reacting with aqueous phase OH radical, with limited aqueous production from HCHO+OH unable to replace HCOOH. The majority of HCOOH depletion occurs from photochemistry during the daytime hours of 15-21 and 30-39including hours 0-7 and 16-25 of the simulations. Both HCOOH and CH_3COOH are greatly underestimated compared to cloud water measurements, similar to the gas phase only results. Model/observational discrepancies are also made worse by the aqueous depletion of HCOOH, suggesting an even greater missing source of gas phase HCOOH, unrepresented aqueous or heterogeneous HCOOH production pathways, or some combination of these processes. These model results imply that gas-to-droplet partitioning is the major source of HCOOH and CH_3COOH in cloud water rather than chemical production within cloud droplets. This is confirmed by comparing the rate of gas-to-droplet partitioning to aqueous production, which is 100x and 10,000x greater for HCOOH and CH_3COOH respectively.

The depletion of HCOOH deviates from a previous cloud chemistry modeling study at WFM (Barth et al., 2021). The same aqueous chemical mechanism found strong production of HCOOH within cloud water due, while a more complex aqueous mechanism, CAPRAM 4.0α exhibited even stronger production due to reactions involving the aqueous oxidation of CH_3CO_3H not included in the model used in this study. The differences in model results on different dates imply that cloud water chemistry can either be a net source or net sink of HCOOH depending on the given scenario. The reasons for HCOOH depletion in this modeling study remains unclear, but likely is related to missing reactions in one or both of the gas and aqueous phases that are beyond the scope of this work.

5 Oxalic Acidacid

Neither MOZART T1 or MCM produce OxAc despite its known prevalence, as there is no known gas phase chemistry that produces OxAc. Current research points to aqueous chemistry being its dominant source, with glyoxal serving as an important precursor (Sorooshian et al., 2006; Lee et al., 2011). Since glyoxal serves as an important precursor gas for organic acid production, it is worth investigating the gas-phase chemistry controlling glyoxal production.

5.1 Glyoxal Production

Glyoxal shows complex differences between the two gas phase mechanisms (Figure11). In the first two sets of trajectories, MCM produces up to 2x more glyoxal than MOZART T1 but for later sets of trajectories, such as 6-29-2018 at 8:00 and 10:00 UTC, MOZART T1 produces up to 50 pptv more glyoxal than MCM. The higher glyoxal mixing ratios within MOZART T1 are associated with higher daytime isoprene mixing ratios (greater than 1 ppbv) coupled with higher NO_x mixing ratios over the Chicago Metropolitan area. Further investigation of the major chemical production pathways between the two mechanisms reveals that MCM predicts considerable ozonolysis chemistry of isoprene oxidation products (including a strong source from

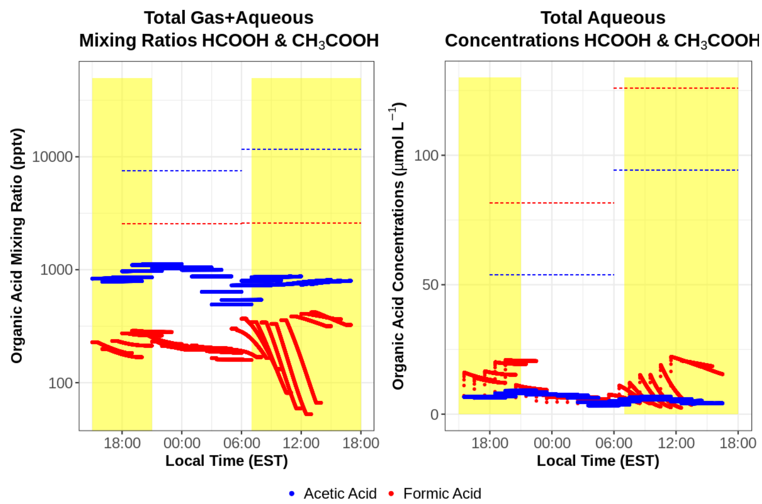

Figure 10. Total (gas + aqueous) mixing ratios (left) and aqueous phase concentrations (right) of HCOOH (red) and CH_3COOH (blue) from the simple gas + aqueous box model run at the summit of WFM during a cloud event that occurred from June 30th to July 1st, 2018. Dashed horizontal lines represent cloud water concentrations measured at WFM during this period. Total mixing ratios in the left plot were derived from the cloud water measurements using Eqs. 1-3.

the ozonolysis of a hydroperoxy aldehyde or C5HPALD2 in MCMv3.3.1), a source that is not included in MOZART T1 (shown in Figure ~~S20~~S23). Trajectories launched on 2018-06-28 22:00 UTC show the strongest nocturnal production within MCMv 3.3.1 as the simulation starts towards the end of the day. Photochemistry only has a few hours to oxidize nearly 5 ppbv of isoprene, and as a results only produces typically short-lived second-generation oxidation products such as C5HPALD2 (with a chemical lifetime of 1 hour when OH = 5x10^6 molecules cm^{-3} s^{-1}), which then strongly reacts with O_3 at night to form glyoxal.

In trajectories influenced by anthropogenic NO_x, such as ensembles launched on 6/29/18 6:00 UTC and 10:00 UTC, a major glyoxal production pathway in MOZART T1 is the reaction of a lumped peroxy radical (XO_2) with NO, where XO_2 is a lumped species representing peroxy radicals formed in the oxidation of isoprene by-products including isoprene epoxydiol (IEPOX), hydroperoxyaldehyde (HPALD), and an a unsaturated hydroxyhydroperoxide (ISOPOOH), and represents the daytime chemistry that leads to greater glyoxal production in MOZART T1 compared to MCMv 3.3.1. Similar to CH_3COOH, the disagreements between the two mechanisms largely disappear for glyoxal as trajectories arrive at WFM, as primary VOCs are depleted and glyoxal is oxidized or the air parcel entrains background air (Figure ~~S21~~S24).

5.2 Oxalic acid cloud chemistry

Results of the gas + aqueous modeling find substantial aqueous phase production of OxAc that corresponds with a sharp aqueous phase depletion of glyoxal (Figure 12). OxAc production is confined to the daytime, as the OH radical is the major driver of OxAc production chemistry within the model. The concentrations of OxAc are well within an order of magnitude of

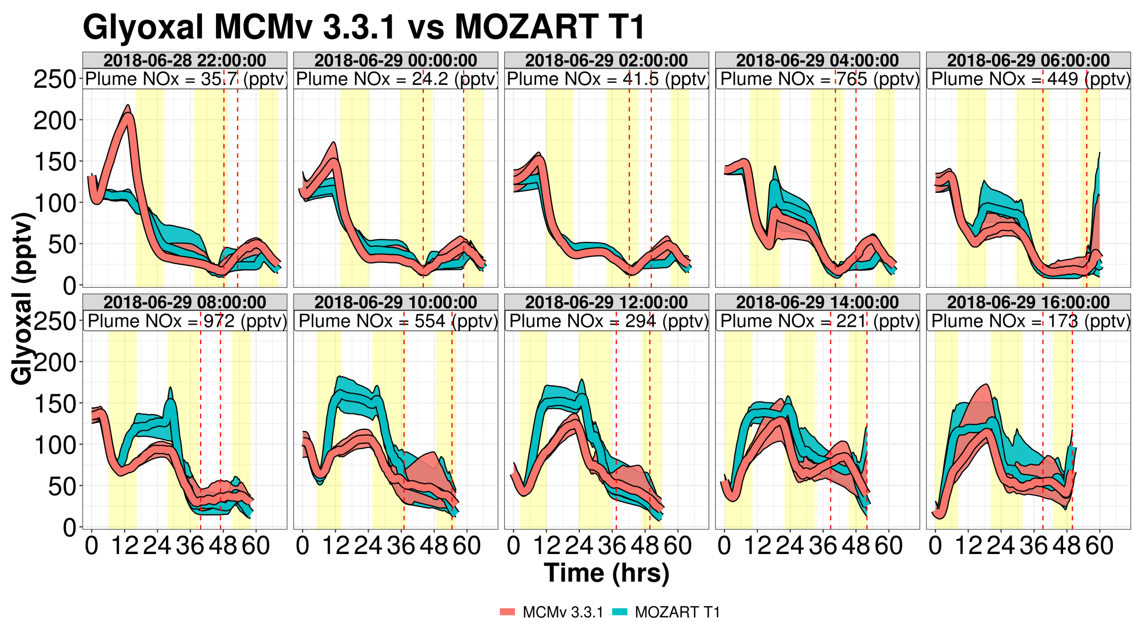

Figure 11. Same as Figure 7 but for glyoxal

measured cloud water concentrations. These simulations suggest that aqueous chemistry of small carbonyl compounds such as glyoxal can largely explain the observed concentration of organic acids such as OxAc. It is important to note that this is a simplified aqueous box model that focuses on 2 or 3 carbon organic acid chemistry that is better suited for chemical transport models. There are aqueous chemical mechanisms that contain larger organic compounds and more aqueous phase reactions that likely better capture the chemical complexity in cloud droplets and wet aerosol (McNeill et al., 2012; Mouchel-Vallon et al., 2017; Bräuer et al., 2019). Additionally, other types of chemistry such a transition metal ion chemistry (Zuo and Hoigne, 1992; Sorooshian et al., 2013) or reactions involving organic nitrogen or organic sulfur compounds (Pratt et al., 2013; Lim et al., 2016) are not included in this mechanism that could have direct or indirect impacts on organic acid formation. Uncertainties of Henry's Law for OxAc and precursor gases may also contribute to uncertainties in overall OxAc production. Despite these uncertainties, the model results provide strong evidence that under atmospherically relevant conditions, aqueous chemistry can have major impacts on concentrations of organic acids like OxAc and HCOOH.

6 Discussion

6.1 Influence of anthropogenic NO_x emissions on organic acid formation

~~Model predictions suggest strong~~ Strong isoprene emissions from Missouri are a major contributor to all three organic acids discussed in this work. However, several air parcels modeled in this study are also influenced by anthropogenic NO_x emissions from the Chicago metropolitan area, which impacted the oxidation pathway of isoprene in these simulations. A high NO_x

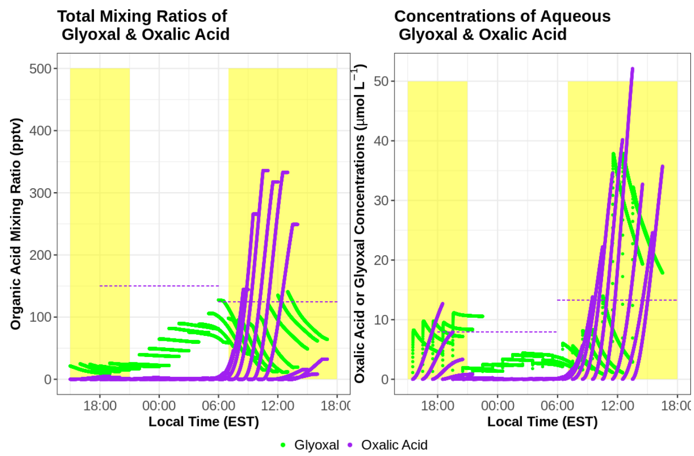

Figure 12. Same as Figure 10 but for glyoxal (green) and OxAc (purple). Dashed horizontal lines represent observations from WFM cloud water.

versus low NO_x chemical regime for specific VOCs is often defined by whether RO_2 predominately reacts with NO or HO_2, which can change the overall oxidation pathway of the VOC. The [NO]/[HO_2] ratio can serve as a useful proxy for the NO_x regime to explore the impacts of anthropogenic NO_x on organic acid production. The impact of NO_x emissions from the Chicago Metropolitan area on HCOOH production are subtle, as the dominant production pathway of HCOOH is from isoprene ozonolysis. NO_x, coupled with warm temperatures, is directly related to O_3 production and high NO_x could therefore contribute indirectly to HCOOH formation. However there ~~is little correlation~~ very little connection between [NO]/[HO_2] ratios with HCOOH production rates in these simulations (Figure ~~S22~~S25), as the vast majority of HCOOH production in all trajectory ensembles occurred during the first 10-15 hours of the simulation, before trajectories reached the Chicago Metropolitan Area and the primary VOCs responsible for HCOOH production (mainly isoprene) are largely exhausted. NO_x emissions have a more direct impact on CH_3COOH production, particularly within MCM, with the production of CH_3COOH being reduced by up to 3x for [NO]/[HO_2] ratios greater than 10 (Figure ~~S23~~S26). This reduction is caused by NO out-competing HO_2 and RO_2 to react with CH_3CO_3 due to elevated anthropogenic NO_x emissions from the Chicago Metropolitan Area, thus reducing the major production pathway of CH_3COOH. However, like HCOOH, there majority of production of CH_3COOH occurs before the trajectories arrive in Chicago, muting the NO_x impact on overall production.

It is not possible to directly investigate the role of anthropogenic NO_x on OxAc using these simulations, as there is no gas phase production of OxAc in either mechanism. Instead, glyoxal's NO_x dependency can be examined as a proxy for OxAc. Both gas phase mechanisms show glyoxal production increasing with [NO]/[HO_2] ratios, with a stronger relationship within MOZART T1 simulations, due to the parameterized XO_2 +NO reaction (Figure ~~S24~~S27). The timing of the NO_x emissions is as important as the strength of the emission sources as it relates to glyoxal. The trajectory ensemble launched on 06/29/2018 8:00 UTC exhibited some of the highest NO_x mixing ratios (>2 ppbv) in the simulations~~(Figure S11~~, (Figure S14), but these emissions arrived mostly at night, muting the impact they could have on glyoxal production. Compare this to the trajectories launched on 06/29/2018 10:00 UTC, where anthropogenic NO_x contributes to a glyoxal production rate 2 times greater than the 06/29/2018 8:00 UTC trajectories in the first 40 hours of the simulations, despite NO_x mixing ratios being approximately 2 times smaller. These results indicate daytime anthropogenic influence increased overall glyoxal production and its likely oxidation products such as oxalic acid, but this influence was decreased due to the timing of the NO_x emissions.

6.2 Modeling Uncertainties

There are several processes that may contribute to uncertainties in modeling organic acids that arise from unknowns in both gas-phase and aqueous-phase chemistry as well as the lack of measurements of a suite of trace gases and aerosol composition and concentrations. There are large disagreements between MOZART T1 and MCMv 3.3.1 in the production of CH_3COOH and glyoxal. While there is mechanism agreement as trajectories arrive at WFM, this agreement is caused by entrainment of background air controlling the CH_3COOH and glyoxal mixing ratios rather than similar chemical production rates. Investigating the production of these gases in another location or on a different date would likely lead to different results. While changing the entrainment parameter within the box modeling did not impact the conclusions of this work, changes in this parameter did have an appreciable impact on the magnitude of the organic acid mixing ratios, and thus increasing the uncertainty in modeling organic acid production. The model runs underestimating HCOOH and CH_3COOH by an order of magnitude imply missing chemistry, but it is unclear if this is due to gas and/or aqueous chemistry.

While the gas+aqueous chemistry model produces measured OxAC concentrations, the model is missing known processes that could serve as OxAc sources such as the oxidation of larger organic compounds (Tilgner and Herrmann, 2010; Barth et al., 2021), sinks such as iron-oxalate complexes (Zuo and Hoigne, 1992; Sorooshian et al., 2013; Mouchel-Vallon et al., 2017), or key controls of the oxidant budget like photo-fenton reactions (Deguillaume et al., 2005; Nguyen et al., 2013))

The box model simulations also lack representation of organic aerosol that may contribute further uncertain. Organic acids may have already existed within aerosol before cloud formation, providing a direct source of organic acids to cloud water before any chemistry has occurred. Carbonyl compounds have also been detected within aerosol samples (Liu et al., 2022; Wang et al., 2022) , which can be then oxidized after cloud droplet activation to form organic acids. WSOC can serve as an important sink for aqueous-phase OH, which can either enhance or reduce organic acid production depending on the amount of organic acid precursors available for reaction (Arakaki et al., 2013; Tilgner and Herrmann, 2018).

In addition to uncertainties of modeling components, the lack of field observations of both organic acids and their precursors reduces our ability to constrain organic acid production. Regular monitoring of organic acids and their precursor gases are rare in the Northeast US or elsewhere. VOCs are monitored in networks like the EPA's Photochemical Assessment Monitoring Stations (PAMS), but are designed to assess O_3 production, and are therefore constrained to more populated regions . Whiteface Mountain is the only site in the region that monitors organic acids and there are no recent gas phase organic acid measurements in the region, with the most recent known measurements occurring in 1991 (Khwaja, 1995).

6.3 Future Work

Future work will investigate the impacts of cloud water chemistry on organic acid production in more detail. Specific attention will be paid to the aqueous phase depletion of HCOOH and why this result differs from a another WFM case study using the same mechanism (Barth et al., 2021). In addition to a more detailed look at the key chemical reactions (ie sinks, sources, oxidant budgets) within the simple gas+aqueous phase mechanism, the aqueous chemistry will be expanded to include key processes that were not represented in this work, including metal-organic complexes and associated photo-chemistry, photo-fenton chemistry, and the inclusion of larger organic compounds in the mechanisms. This updated chemistry will then be compared to observations to see if the improved mechanism can better describe HCOOH, CH_3COOH, and OxAc concentrations.

7 Summary and Conclusions

This study used a combination of WRF-Chem and Lagrangian chemical box modeling to investigate the major chemical processes that impact organic acid formation in both the gas and aqueous phases at Whiteface Mountain, NY (WFM) during a pollution event on July 1, 2018 that led to record high organic acid concentrations. HYSPLIT ensemble back-trajectory analysis determined that WFM received influence from Central Missouri, a region with strong biogenic VOC emissions, and anthropogenic emissions from Chicago Metropolitan Area. WRF-Chem simulations were used to simulate before and during the pollution, and to launch forward trajectories based on the HYSPLIT results. WRF-Chem was then used to provide input necessary for chemical box modeling along the trajectories. To determine if gas-phase chemistry can explain the organic acid concentrations measured at WFM, the box model, BOXMOX, was run with two gas phase mechanisms (the Model for OZone and Related Tracers or MOZART T1 and the Master Chemical Mechanism or MCMv3.3.1) The MOZART T1 mechanism is a condensed gas-phase mechanism while MCMv 3.3.1 is more detailed, allowing evaluation of whether MOZART T1 can sufficiently predict organic acid production compared to MCMv 3.3.1. The gas phase box model results were then used as input for a simple gas+aqueous box model run at the summit of WFM to investigate the potential role of aqueous chemistry on organic acids. Strong biogenic emissions of isoprene from Missouri driven by a heat wave were responsible for the strong production of organic acids, with influence from anthropogenic inputs of NO_x from the Chicago metropolitan area.

The two gas phase mechanisms used in the BOXMOX simulations showed good agreement in HCOOH production, with ozonolysis chemistry from isoprene, MACR, and MVK serving as the major sources. MCMv 3.3.1 produced up to 40% more CH_3COOH than MOZART T1 under high isoprene but low NO_x conditions due a stronger CH_3CO_3+ HO_2 chemical pathway. The two gas phase mechanisms differed in their calculation of glyoxal production. MCMv3.3.1 produced more glyoxal from the nocturnal ozonolysis of hydroperoxy aldehyde or C5HPALD2, a low NOx oxidation product of isoprene, while MOZART T1 produced more glyoxal under higher NO_x conditions where NO + XO_2 dominated. The disagreements between the two mechanisms for CH_3COOH and glyoxal largely disappear as they arrive at WFM, but this is due the entrainment of background air dominating mixing ratios after emitted primary VOCs have been exhausted. Both gas phase mechanisms greatly underpredicted HCOOH and CH_3COOH by an order of magnitude in comparison to measurements made a WFM.

To learn how aqueous-phase chemistry could contribute to organic acid formation, a cloud chemistry box model was applied using a simple aqueous-phase mechanism. The gas+aqueous phase box model shows little change in CH_3COOH mixing ratios due to aqueous chemistry but exhibits a significant depletion of HCOOH, exacerbating the gas phase underpredictions of HCOOH. Glyoxal mixing ratios showed ~~strong disagreements between~~ of up to 100 pptv between the two mechanisms upwind of WFM, with MCMv 3.3.1 producing large ~~amount~~ 50-100 pptv of glyoxal at nighttime from the ozonolysis of an isoprene hydroperoxy aldehyde (C5HPALD2), while MOZART T1 showed ~~stronger production~~ 2x greater production of glyoxal during the day from the lumped isoprene oxidation peroxy radical XO_2 reaction with NO. Anthropogenic NO_x emissions led to increased glyoxal production in both mechanisms, but the effect was stronger within MOZART T1. There is strong aqueous production of OxAc from carbonyl compounds like glyoxal, with concentrations well within an order of magnitude of cloud water measurements at WFM. The gas+aqueous box modeling indicates that aqueous processing can impact organic acid concentrations.

These results contribute to ~~a growing body of work showing the large uncertainties in modeling organic acids . Furthermore, only a~~ the limited research indicating that biogenic VOC emissions are a major source of organic acids in the atmosphere but gas phase chemistry alone greatly underpredict their atmospheric concentrations. While the addition of aqueous chemistry does not improve the model predictions of HCOOH and CH_3COOH , this study provides further evidence that cloud droplets are a major source of oxalic acid under realistic atmospheric conditions. Only a limited number of modeling studies have looked explicitly at OxAc, (Crahan et al., 2004; Ervens et al., 2004; Warneck, 2005; Chen et al., 2007; Myriokefalitakis et al., 2011; Zhu et al., 2019; Barth et al., 2021; Myriokefalitakis et al., 2022) , despite its role as a significant component of SOA mass. A major reason for this is that most chemical transport models contain either no or a crude representation of organic chemistry within cloud droplets. The lack of representation of aqueous organic chemistry risks the model developing a "clear sky bias", phrase introduced in Christiansen et al. (2020), preventing proper characterization of the chemical properties of organic aerosol. ~~Mechanism development and deployment within these models is necessary to better simulate organic acids concentrations and organic aerosol.~~

~~Another~~ A large contributing factor to uncertainties in organic acid production is the lack of observational data, particularly organic acids in both the gas and aqueous phases. Regular observational studies over a broader range of geographical and temporal scales are required to better constrain organic ~~acids~~acid concentrations. VOC measurements of key organic acid precursors like isoprene, methacrolein, methyl vinyl ketone, and glyoxal, especially in regions of high BVOC emissions, are ~~required~~ needed to better constrain organic acid production. Cloud water chemistry measurements ~~need~~ must to be expanded beyond organic acids to include key aqueous precursor gases such as glyoxal and methylglyoxal. Simultaneous gas and aqueous phase field measurements are also necessary, as cloud water measurements alone are not sufficient to properly investigate cloud water processing of organic carbon. Finally modeling work at different temporal and geographic scales coupled with field observations is necessary for ~~advances in model development and to better understand~~ improved modeling of organic acids so that the processes governing atmospheric chemistry are better represented. The procedure of back-trajectory analysis that then initialize forward trajectory runs within WRF-Chem (or another chemical transport model) could be automated to provide insight to researchers during field campaigns and guide laboratory analysis of collected samples to target specific chemical species or processes.

The Northeast US is a region undergoing a significant shift in condensed phase chemical composition from a SO_4^{2-} and NO_3^- dominated system to an organic carbon dominated system, with organic acids representing a larger fraction of total ions in cloud and rain water (Lawrence et al., 2023) . Because of the trend towards a higher fraction of organic acids in cloud water, it is critical to better understand their production. As the world decarbonizes and anthropogenic emissions of SO_2 and NO_x decrease, field campaigns and modeling efforts targeting the Northeast US can serve as a blueprint for other regions of the world that are experiencing similar changes in atmospheric composition and chemistry, improving the representation in air quality and climate models of aerosol and precipitation composition and therefore inform policy decisions.

Author contributions. E. Yerger and D. Kelting conducted the cloud water chemical analysis. P. Casson, R.Brandt, C.Lawrence and S.Lance conducted the cloud water sampling in 2018. M. Barth and C.Lawrence conducted WRF-Chem simulations. C.Lawrence conducted box modeling simulations. J.Orlando consulted on box model results. C.Lawrence and M.Barth wrote the manuscript with contributions from all co-authors.

Competing interests. The authors have the following competing interests: At least one of the (co-)authors is a member of the editorial board of Atmospheric Chemistry and Physics.

Acknowledgements. The NSF National Center for Atmospheric Research (NCAR) is a major facility sponsored by the U.S. National Science Foundation under Cooperative Agreement No. 1852977. The authors would like to thank the NCAR Advanced Studies Program Graduate Visitor Program and NCAR's Atmospheric Chemistry Observations and Modeling Laboratory for providing travel funding to allow in person collaboration between authors C. Lawrence, M. Barth, and J.Orlando. We would like to acknowledge the high-performance computing support from Cheyenne (doi:10.5065/D6RX99HX) provided by NSF NCAR's Computational and Information Systems Laboratory. We acknowledge use of the WRF-Chem preprocessors tool (mozbc, fire_emiss, biogenic emissions, anthropogenic emissions), provided by NSF NCAR/ACOM. C.Lawrence's graduate research is funded by NASA's Future Investigators in NASA Earth and Space Science and Technology (FINESST) program (award number 80NSSC21K1633) and the NSF's Faculty Early Career Development (CAREER) grant (award number 1945563). Cloud water measurements reported in this paper were supported by the New York State Energy Research and Development Authority (NYSERDA) Contract 124461 (2018-2021). We would also like to thank James Schwab for providing trace gas data from Whiteface Mountain, Pinnacle State Park, and Queens College. WFM trace gas and meteorological measurements were supported by NYSERDA Contract 48971. NYSERDA has not reviewed the information contained herein, and the opinions expressed in this report do not necessarily reflect those of NYSERDA or the State of New York.

References

Arakaki, T., Anastasio, C., Kuroki, Y., Nakajima, H., Okada, K., Kotani, Y., Handa, D., Azechi, S., Kimura, T., Tsuhako, A., and Miyagi, Y.: A General Scavenging Rate Constant for Reaction of Hydroxyl Radical with Organic Carbon in Atmospheric Waters, Environmental Science & Technology, 47, 8196–8203, https://doi.org/10.1021/es401927b, publisher: American Chemical Society, 2013.

Avery, G. B., Tang, Y., Kieber, R. J., and Willey, J. D.: Impact of recent urbanization on formic and acetic acid concentrations in coastal North Carolina rainwater, Atmospheric Environment, 35, 3353–3359, https://doi.org/10.1016/S1352-2310(00)00328-9, 2001.

Barth, M. C., Ervens, B., Herrmann, H., Tilgner, A., McNeill, V. F., Tsui, W. G., Deguillaume, L., Chaumerliac, N., Carlton, A., and Lance, S. M.: Box Model Intercomparison of Cloud Chemistry, Journal of Geophysical Research: Atmospheres, 126, e2021JD035 486, https://doi.org/10.1029/2021JD035486, _eprint: https://onlinelibrary.wiley.com/doi/pdf/10.1029/2021JD035486, 2021.

Berasategui, M., Amedro, D., Vereecken, L., Lelieveld, J., and Crowley, J. N.: Reaction between $CH_3C(O)OOH$ (peracetic acid) and OH in the gas phase: a combined experimental and theoretical study of the kinetics and mechanism, Atmospheric Chemistry and Physics, 20, 13 541–13 555, https://doi.org/10.5194/acp-20-13541-2020, publisher: Copernicus GmbH, 2020.

Blando, J. D. and Turpin, B. J.: Secondary organic aerosol formation in cloud and fog droplets: a literature evaluation of plausibility, Atmospheric Environment, 34, 1623–1632, https://doi.org/10.1016/S1352-2310(99)00392-1, 2000.

Brandt, R. E., Schwab, J. J., Casson, P. W., Roychowdhury, U. K., Wolfe, D., Demerjian, K. L., Civerolo, K. L., Rattigan, O. V., and Felton, H. D.: Atmospheric Chemistry Measurements at Whiteface Mountain, NY: Ozone and Reactive Trace Gases, Aerosol and Air Quality Research, 16, 873–884, https://doi.org/10.4209/aaqr.2015.05.0376, publisher: Taiwan Association for Aerosol Research, 2016.

Bräuer, P., Mouchel-Vallon, C., Tilgner, A., Mutzel, A., Böge, O., Rodigast, M., Poulain, L., van Pinxteren, D., Wolke, R., Aumont, B., and Herrmann, H.: Development of a protocol for the auto-generation of explicit aqueous-phase oxidation schemes of organic compounds, Atmospheric Chemistry and Physics, 19, 9209–9239, https://doi.org/10.5194/acp-19-9209-2019, publisher: Copernicus GmbH, 2019.

Carlton, A. G. and Baker, K. R.: Photochemical Modeling of the Ozark Isoprene Volcano: MEGAN, BEIS, and Their Impacts on Air Quality Predictions, Environmental Science & Technology, 45, 4438–4445, https://doi.org/10.1021/es200050x, publisher: American Chemical Society, 2011.

Carlton, A. G., Turpin, B. J., Altieri, K. E., Seitzinger, S., Reff, A., Lim, H.-J., and Ervens, B.: Atmospheric oxalic acid and SOA production from glyoxal: Results of aqueous photooxidation experiments, Atmospheric Environment, 41, 7588–7602, https://doi.org/10.1016/j.atmosenv.2007.05.035, 2007.

Chaliyakunnel, S., Millet, D., Wells, K., Cady-Pereira, K., and Shephard, M.: A Large Underestimate of Formic Acid from Tropical Fires: Constraints from Space-Borne Measurements, Environmental Science & Technology, 50, 5631–5640, https://doi.org/10.1021/acs.est.5b06385, 2016.

Chen, J., Griffin, R. J., Grini, A., and Tulet, P.: Modeling secondary organic aerosol formation through cloud processing of organic compounds, Atmospheric Chemistry and Physics, 7, 5343–5355, https://doi.org/10.5194/acp-7-5343-2007, publisher: Copernicus GmbH, 2007.

Chen, X., Millet, D. B., Neuman, J. A., Veres, P. R., Ray, E. A., Commane, R., Daube, B. C., McKain, K., Schwarz, J. P., Katich, J. M., Froyd, K. D., Schill, G. P., Kim, M. J., Crounse, J. D., Allen, H. M., Apel, E. C., Hornbrook, R. S., Blake, D. R., Nault, B. A., Campuzano-Jost, P., Jimenez, J. L., and Dibb, J. E.: HCOOH in the Remote Atmosphere: Constraints from Atmospheric Tomography (ATom) Airborne Observations, ACS Earth and Space Chemistry, 5, 1436–1454, https://doi.org/10.1021/acsearthspacechem.1c00049, publisher: American Chemical Society, 2021.

Chen, Y., Hobbs, B. F., Hugh Ellis, J., Crowley, C., and Joutz, F.: Impacts of climate change on power sector NOx emissions: A long-run analysis of the US mid-atlantic region, Energy Policy, 84, 11–21, https://doi.org/10.1016/j.enpol.2015.04.013, 2015.

Christiansen, A. E., Carlton, A. G., and Henderson, B. H.: Differences in fine particle chemical composition on clear and cloudy days, Atmospheric Chemistry and Physics, 20, 11 607–11 624, https://doi.org/10.5194/acp-20-11607-2020, publisher: Copernicus GmbH, 2020.

Crahan, K. K., Hegg, D., Covert, D. S., and Jonsson, H.: An exploration of aqueous oxalic acid production in the coastal marine atmosphere, Atmospheric Environment, 38, 3757–3764, https://doi.org/10.1016/j.atmosenv.2004.04.009, 2004.

Decker, Z. C. J., Zarzana, K. J., Coggon, M., Min, K.-E., Pollack, I., Ryerson, T. B., Peischl, J., Edwards, P., Dubé, W. P., Markovic, M. Z., Roberts, J. M., Veres, P. R., Graus, M., Warneke, C., de Gouw, J., Hatch, L. E., Barsanti, K. C., and Brown, S. S.: Nighttime Chemical Transformation in Biomass Burning Plumes: A Box Model Analysis Initialized with Aircraft Observations, Environmental Science & Technology, 53, 2529–2538, https://doi.org/10.1021/acs.est.8b05359, publisher: American Chemical Society, 2019.

Deguillaume, L., Leriche, M., and Chaumerliac, N.: Impact of radical versus non-radical pathway in the Fenton chemistry on the iron redox cycle in clouds, Chemosphere, 60, 718–724, https://doi.org/10.1016/j.chemosphere.2005.03.052, 2005.

Eger, P. G., Schuladen, J., Sobanski, N., Fischer, H., Karu, E., Williams, J., Riva, M., Zha, Q., Ehn, M., Quéléver, L. L. J., Schallhart, S., Lelieveld, J., and Crowley, J. N.: Pyruvic acid in the boreal forest: gas-phase mixing ratios and impact on radical chemistry, Atmospheric Chemistry and Physics, 20, 3697–3711, https://doi.org/10.5194/acp-20-3697-2020, publisher: Copernicus GmbH, 2020.

Emmons, L. K., Schwantes, R. H., Orlando, J. J., Tyndall, G., Kinnison, D., Lamarque, J.-F., Marsh, D., Mills, M. J., Tilmes, S., Bardeen, C., Buchholz, R. R., Conley, A., Gettelman, A., Garcia, R., Simpson, I., Blake, D. R., Meinardi, S., and Pétron, G.: The Chemistry Mechanism in the Community Earth System Model Version 2 (CESM2), Journal of Advances in Modeling Earth Systems, 12, e2019MS001 882, https://doi.org/10.1029/2019MS001882, _eprint: https://onlinelibrary.wiley.com/doi/pdf/10.1029/2019MS001882, 2020.

EPA, U.: Air Quality System Data Mart, http://www.epa.gov/ttn/airs/aqsdatamar, 2024.

Ervens, B., George, C., Williams, J. E., Buxton, G. V., Salmon, G. A., Bydder, M., Wilkinson, F., Dentener, F., Mirabel, P., Wolke, R., and Herrmann, H.: CAPRAM 2.4 (MODAC mechanism): An extended and condensed tropospheric aqueous phase mechanism and its application, Journal of Geophysical Research: Atmospheres, 108, https://doi.org/10.1029/2002JD002202, 2003.

Ervens, B., Feingold, G., Frost, G. J., and Kreidenweis, S. M.: A modeling study of aqueous production of dicarboxylic acids: 1. Chemical pathways and speciated organic mass production, Journal of Geophysical Research: Atmospheres, 109, https://doi.org/10.1029/2003JD004387, _eprint: https://onlinelibrary.wiley.com/doi/pdf/10.1029/2003JD004387, 2004.

Fast, J. D., Gustafson Jr., W. I., Easter, R. C., Zaveri, R. A., Barnard, J. C., Chapman, E. G., Grell, G. A., and Peckham, S. E.: Evolution of ozone, particulates, and aerosol direct radiative forcing in the vicinity of Houston using a fully coupled meteorology-chemistry-aerosol model, Journal of Geophysical Research: Atmospheres, 111, https://doi.org/10.1029/2005JD006721, _eprint: https://onlinelibrary.wiley.com/doi/pdf/10.1029/2005JD006721, 2006.

Feltracco, M., Barbaro, E., Spolaor, A., Vecchiato, M., Callegaro, A., Burgay, F., Vardè, M., Maffezzoli, N., Dallo, F., Scoto, F., Zangrando, R., Barbante, C., and Gambaro, A.: Year-round measurements of size-segregated low molecular weight organic acids in Arctic aerosol, Science of The Total Environment, 763, 142 954, https://doi.org/10.1016/j.scitotenv.2020.142954, 2021.

Franco, B., Blumenstock, T., Cho, C., Clarisse, L., Clerbaux, C., Coheur, P.-F., De Mazière, M., De Smedt, I., Dorn, H.-P., Emmerichs, T., Fuchs, H., Gkatzelis, G., Griffith, D. W. T., Gromov, S., Hannigan, J. W., Hase, F., Hohaus, T., Jones, N., Kerkweg, A., Kiendler-Scharr, A., Lutsch, E., Mahieu, E., Novelli, A., Ortega, I., Paton-Walsh, C., Pommier, M., Pozzer, A., Reimer, D., Rosanka, S., Sander, R., Schneider, M., Strong, K., Tillmann, R., Van Roozendael, M., Vereecken, L., Vigouroux, C., Wahner, A., and Taraborrelli, D.: Ubiquitous atmospheric production of organic acids mediated by cloud droplets, Nature, 593, 233–237, https://doi.org/10.1038/s41586-021-03462-x, bandiera_abtest: a Cc_license_type: cc_by Cg_type: Nature Research Journals Number: 7858 Primary_atype: Research Publisher: Nature Publishing Group Subject_term: Atmospheric chemistry Subject_term_id: atmospheric-chemistry, 2021.

Fulgham, S. R., Brophy, P., Link, M., Ortega, J., Pollack, I., and Farmer, D. K.: Seasonal Flux Measurements over a Colorado Pine Forest Demonstrate a Persistent Source of Organic Acids, ACS Earth and Space Chemistry, 3, 2017–2032, https://doi.org/10.1021/acsearthspacechem.9b00182, 2019.

Giovannini, L., Ferrero, E., Karl, T., Rotach, M. W., Staquet, C., Trini Castelli, S., and Zardi, D.: Atmospheric Pollutant Dispersion over Complex Terrain: Challenges and Needs for Improving Air Quality Measurements and Modeling, Atmosphere, 11, 646, https://doi.org/10.3390/atmos11060646, number: 6 Publisher: Multidisciplinary Digital Publishing Institute, 2020.

Graedel, T. E. and Eisner, T.: Atmospheric formic acid from formicine ants: a preliminary assessment, Tellus B, 40B, 335–339, https://doi.org/10.1111/j.1600-0889.1988.tb00107.x, 1988.

Grell, G. A., Peckham, S. E., Schmitz, R., McKeen, S. A., Frost, G., Skamarock, W. C., and Eder, B.: Fully coupled "online" chemistry within the WRF model, Atmospheric Environment, 39, 6957–6975, https://doi.org/10.1016/j.atmosenv.2005.04.027, 2005.

Herckes, P., Valsaraj, K. T., and Collett, J. L.: A review of observations of organic matter in fogs and clouds: Origin, processing and fate, Atmospheric Research, 132-133, 434–449, https://doi.org/10.1016/j.atmosres.2013.06.005, 2013.

Jenkin, M. E., Young, J. C., and Rickard, A. R.: The MCM v3.3.1 degradation scheme for isoprene, Atmospheric Chemistry and Physics, 15, 11 433–11 459, https://doi.org/10.5194/acp-15-11433-2015, publisher: Copernicus GmbH, 2015.

Jones, B. T., Muller, J., O'Shea, S., Bacak, A., Allen, G., Gallagher, M., Bower, K., Le Breton, M., Bannan, T. J., Bauguitte, S., Pyle, J., Lowry, D., Fisher, R., France, J., Nisbet, E., Shallcross, D., and Percival, C.: Are the Fenno-Scandinavian Arctic Wetlands a Significant Regional Source of Formic Acid?, Atmosphere, 8, 112, https://doi.org/10.3390/atmos8070112, 2017.

Kawamura, K. and Bikkina, S.: A review of dicarboxylic acids and related compounds in atmospheric aerosols: Molecular distributions, sources and transformation, Atmospheric Research, 170, 140–160, https://doi.org/10.1016/j.atmosres.2015.11.018, 2016.

Kawamura, K., Hoque, M. M. M., Bates, T. S., and Quinn, P. K.: Molecular distributions and isotopic compositions of organic aerosols over the western North Atlantic: Dicarboxylic acids, related compounds, sugars, and secondary organic aerosol tracers, Organic Geochemistry, 113, 229–238, https://doi.org/10.1016/j.orggeochem.2017.08.007, tex.ids= kawamuraMolecularDistributionsIsotopic2017, 2017.

Khwaja, H. A.: Atmospheric concentrations of carboxylic acids and related compounds at a semiurban site, Atmospheric Environment, 29, 127–139, https://doi.org/10.1016/1352-2310(94)00211-3, 1995.

Knote, C., Tuccella, P., Curci, G., Emmons, L., Orlando, J. J., Madronich, S., Baró, R., Jiménez-Guerrero, P., Luecken, D., Hogrefe, C., Forkel, R., Werhahn, J., Hirtl, M., Pérez, J. L., San José, R., Giordano, L., Brunner, D., Yahya, K., and Zhang, Y.: Influence of the choice of gas-phase mechanism on predictions of key gaseous pollutants during the AQMEII phase-2 intercomparison, Atmospheric Environment, 115, 553–568, https://doi.org/10.1016/j.atmosenv.2014.11.066, 2015.

Kumar, M., Burrell, E., Hansen, J. C., and Francisco, J. S.: Molecular insights into organic particulate formation, Communications Chemistry, 2, 1–10, https://doi.org/10.1038/s42004-019-0183-7, number: 1 Publisher: Nature Publishing Group, 2019.

Lawrence, C. E., Casson, P., Brandt, R., Schwab, J. J., Dukett, J. E., Snyder, P., Yerger, E., Kelting, D., VandenBoer, T. C., and Lance, S.: Long-term monitoring of cloud water chemistry at Whiteface Mountain: the emergence of a new chemical regime, Atmospheric Chemistry and Physics, 23, 1619–1639, https://doi.org/10.5194/acp-23-1619-2023, publisher: Copernicus GmbH, 2023.

Lee, A. K. Y., Herckes, P., Leaitch, W. R., Macdonald, A. M., and Abbatt, J. P. D.: Aqueous OH oxidation of ambient organic aerosol and cloud water organics: Formation of highly oxidized products, Geophysical Research Letters, 38, https://doi.org/10.1029/2011GL047439, 2011.

Legrand, M., Gros, V., Preunkert, S., Sarda-Estève, R., Thierry, A.-M., Pépy, G., and Jourdain, B.: A reassessment of the budget of formic and acetic acids in the boundary layer at Dumont d'Urville (coastal Antarctica): The role of penguin emissions on the budget of several oxygenated volatile organic compounds, Journal of Geophysical Research: Atmospheres, 117, https://doi.org/10.1029/2011JD017102, 2012.

Li, Y., Barth, M. C., Patton, E. G., and Steiner, A. L.: Impact of In-Cloud Aqueous Processes on the Chemistry and Transport of Biogenic Volatile Organic Compounds, Journal of Geophysical Research: Atmospheres, 122, 11,131–11,153, https://doi.org/10.1002/2017JD026688, _eprint: https://onlinelibrary.wiley.com/doi/pdf/10.1002/2017JD026688, 2017.

Li, Y., Zhao, J., Wang, Y., Seinfeld, J. H., and Zhang, R.: Multigeneration Production of Secondary Organic Aerosol from Toluene Photooxidation, Environmental Science & Technology, 55, 8592–8603, https://doi.org/10.1021/acs.est.1c02026, publisher: American Chemical Society, 2021.

Lim, H.-J., Carlton, A. G., and Turpin, B. J.: Isoprene Forms Secondary Organic Aerosol through Cloud Processing: Model Simulations, Environmental Science & Technology, 39, 4441–4446, https://doi.org/10.1021/es048039h, publisher: American Chemical Society, 2005.

Lim, Y. B., Tan, Y., and Turpin, B. J.: Chemical insights, explicit chemistry, and yields of secondary organic aerosol from OH radical oxidation of methylglyoxal and glyoxal in the aqueous phase, Atmospheric Chemistry and Physics, 13, 8651–8667, https://doi.org/10.5194/acp-13-8651-2013, publisher: Copernicus GmbH, 2013.

Lim, Y. B., Kim, H., Kim, J. Y., and Turpin, B. J.: Photochemical organonitrate formation in wet aerosols, Atmospheric Chemistry and Physics, 16, 12 631–12 647, https://doi.org/https://doi.org/10.5194/acp-16-12631-2016, publisher: Copernicus GmbH, 2016.

Link, M. F., Nguyen, T. B., Bates, K., Müller, J.-F., and Farmer, D. K.: Can Isoprene Oxidation Explain High Concentrations of Atmospheric Formic and Acetic Acid over Forests?, ACS Earth and Space Chemistry, 4, 730–740, https://doi.org/10.1021/acsearthspacechem.0c00010, publisher: American Chemical Society, 2020.

Link, M. F., Brophy, P., Fulgham, S. R., Murschell, T., and Farmer, D. K.: Isoprene versus Monoterpenes as Gas-Phase Organic Acid Precursors in the Atmosphere, ACS Earth and Space Chemistry, 5, 1600–1612, https://doi.org/10.1021/acsearthspacechem.1c00093, publisher: American Chemical Society, 2021.

Liu, Q., Gao, Y., Huang, W., Ling, Z., Wang, Z., and Wang, X.: Carbonyl compounds in the atmosphere: A review of abundance, source and their contributions to O3 and SOA formation, Atmospheric Research, 274, 106 184, https://doi.org/10.1016/j.atmosres.2022.106184, 2022.

Maia-Silva, D., Kumar, R., and Nateghi, R.: The critical role of humidity in modeling summer electricity demand across the United States, Nature Communications, 11, 1686, https://doi.org/10.1038/s41467-020-15393-8, publisher: Nature Publishing Group, 2020.

McNeill, V. F., Woo, J. L., Kim, D. D., Schwier, A. N., Wannell, N. J., Sumner, A. J., and Barakat, J. M.: Aqueous-Phase Secondary Organic Aerosol and Organosulfate Formation in Atmospheric Aerosols: A Modeling Study, Environmental Science & Technology, 46, 8075–8081, https://doi.org/10.1021/es3002986, 2012.

Mielnik, A., Link, M., Mattila, J., Fulgham, S. R., and Farmer, D. K.: Emission of formic and acetic acids from two Colorado soils, Environmental Science: Processes & Impacts, 20, 1537–1545, https://doi.org/10.1039/C8EM00356D, 2018.

Millet, D. B., Baasandorj, M., Farmer, D. K., Thornton, J. A., Baumann, K., Brophy, P., Chaliyakunnel, S., de Gouw, J. A., Graus, M., Hu, L., Koss, A., Lee, B. H., Lopez-Hilfiker, F. D., Neuman, J. A., Paulot, F., Peischl, J., Pollack, I. B., Ryerson, T. B., Warneke, C., Williams, B. J., and Xu, J.: A large and ubiquitous source of atmospheric formic acid, Atmospheric Chemistry and Physics, 15, 6283–6304, https://doi.org/10.5194/acp-15-6283-2015, publisher: Copernicus GmbH, 2015.

Miyazaki, Y., Aggarwal, S. G., Singh, K., Gupta, P. K., and Kawamura, K.: Dicarboxylic acids and water-soluble organic carbon in aerosols in New Delhi, India, in winter: Characteristics and formation processes, Journal of Geophysical Research: Atmospheres, 114, https://doi.org/10.1029/2009JD011790, 2009.

Mouchel-Vallon, C., Deguillaume, L., Monod, A., Perroux, H., Rose, C., Ghigo, G., Long, Y., Leriche, M., Aumont, B., Patryl, L., Armand, P., and Chaumerliac, N.: CLEPS 1.0: A new protocol for cloud aqueous phase oxidation of VOC mechanisms, Geoscientific Model Development, 10, 1339–1362, https://doi.org/10.5194/gmd-10-1339-2017, publisher: Copernicus GmbH, 2017.

Mungall, E. L., Abbatt, J. P. D., Wentzell, J. J. B., Wentworth, G. R., Murphy, J. G., Kunkel, D., Gute, E., Tarasick, D. W., Sharma, S., Cox, C. J., Uttal, T., and Liggio, J.: High gas-phase mixing ratios of formic and acetic acid in the High Arctic, Atmospheric Chemistry and Physics, 18, 10 237–10 254, https://doi.org/10.5194/acp-18-10237-2018, publisher: Copernicus GmbH, 2018.

Myriokefalitakis, S., Tsigaridis, K., Mihalopoulos, N., Sciare, J., Nenes, A., Kawamura, K., Segers, A., and Kanakidou, M.: In-cloud oxalate formation in the global troposphere: a 3-D modeling study, Atmospheric Chemistry and Physics, 11, 5761–5782, https://doi.org/10.5194/acp-11-5761-2011, publisher: Copernicus GmbH, 2011.

Myriokefalitakis, S., Bergas-Massó, E., Gonçalves-Ageitos, M., Pérez García-Pando, C., van Noije, T., Le Sager, P., Ito, A., Athanasopoulou, E., Nenes, A., Kanakidou, M., Krol, M. C., and Gerasopoulos, E.: Multiphase processes in the EC-Earth model and their relevance to the atmospheric oxalate, sulfate, and iron cycles, Geoscientific Model Development, 15, 3079–3120, https://doi.org/10.5194/gmd-15-3079-2022, publisher: Copernicus GmbH, 2022.

Nguyen, T. B., Coggon, M. M., Flagan, R. C., and Seinfeld, J. H.: Reactive Uptake and Photo-Fenton Oxidation of Glycolaldehyde in Aerosol Liquid Water, Environmental Science & Technology, 47, 4307–4316, https://doi.org/10.1021/es400538j, publisher: American Chemical Society, 2013.

Ninneman, M., Lu, S., Zhou, X., and Schwab, J.: On the Importance of Surface-Enhanced Renoxification as an Oxides of Nitrogen Source in Rural and Urban New York State, ACS Earth and Space Chemistry, 4, 1985–1992, https://doi.org/10.1021/acsearthspacechem.0c00185, publisher: American Chemical Society, 2020.

Pandis, S. N. and Seinfeld, J. H.: Should bulk cloudwater or fogwater samples obey Henry's law?, Journal of Geophysical Research: Atmospheres, 96, 10 791–10 798, https://doi.org/10.1029/91JD01031, _eprint: https://agupubs.onlinelibrary.wiley.com/doi/pdf/10.1029/91JD01031, 1991.

Paulot, F., Wunch, D., Crounse, J. D., Toon, G. C., Millet, D. B., DeCarlo, P. F., Vigouroux, C., Deutscher, N. M., González Abad, G., Notholt, J., Warneke, T., Hannigan, J. W., Warneke, C., de Gouw, J. A., Dunlea, E. J., De Mazière, M., Griffith, D. W. T., Bernath, P., Jimenez, J. L., and Wennberg, P. O.: Importance of secondary sources in the atmospheric budgets of formic and acetic acids, Atmospheric Chemistry and Physics, 11, 1989–2013, https://doi.org/10.5194/acp-11-1989-2011, 2011.

Place, B. K., Hutzell, W. T., Appel, K. W., Farrell, S., Valin, L., Murphy, B. N., Seltzer, K. M., Sarwar, G., Allen, C., Piletic, I. R., D'Ambro, E. L., Saunders, E., Simon, H., Torres-Vasquez, A., Pleim, J., Schwantes, R. H., Coggon, M. M., Xu, L., Stockwell, W. R., and Pye, H. O. T.: Sensitivity of northeastern US surface ozone predictions to the representation of atmospheric chemistry in the Community Regional Atmospheric Chemistry Multiphase Mechanism (CRACMMv1.0), Atmospheric Chemistry and Physics, 23, 9173–9190, https://doi.org/10.5194/acp-23-9173-2023, publisher: Copernicus GmbH, 2023.

Pratt, K. A., Fiddler, M. N., Shepson, P. B., Carlton, A. G., and Surratt, J. D.: Organosulfates in cloud water above the Ozarks' isoprene source region, Atmospheric Environment, 77, 231–238, https://doi.org/10.1016/j.atmosenv.2013.05.011, 2013.

Pye, H. O. T., Nenes, A., Alexander, B., Ault, A. P., Barth, M. C., Clegg, S. L., Collett Jr., J. L., Fahey, K. M., Hennigan, C. J., Herrmann, H., Kanakidou, M., Kelly, J. T., Ku, I.-T., McNeill, V. F., Riemer, N., Schaefer, T., Shi, G., Tilgner, A., Walker, J. T., Wang, T., Weber, R., Xing, J., Zaveri, R. A., and Zuend, A.: The acidity of atmospheric particles and clouds, Atmospheric Chemistry and Physics, 20, 4809–4888, https://doi.org/https://doi.org/10.5194/acp-20-4809-2020, publisher: Copernicus GmbH, 2020.

Sander, R.: Compilation of Henry's law constants (version 5.0.0) for water as solvent, Atmospheric Chemistry and Physics, 23, 10 901–12 440, https://doi.org/10.5194/acp-23-10901-2023, publisher: Copernicus GmbH, 2023.

Schwab, J. J., Casson, P., Brandt, R., Husain, L., Dutkewicz, V., Wolfe, D., Demerjian, K. L., Civerolo, K. L., Rattigan, O. V., Felton, H. D., and Dukett, J. E.: Atmospheric Chemistry Measurements at Whiteface Mountain, NY: Cloud Water Chemistry, Precipitation Chemistry, and Particulate Matter, Aerosol and Air Quality Research, 16, 841–854, https://doi.org/10.4209/aaqr.2015.05.0344, publisher: Taiwan Association for Aerosol Research, 2016.

Schwantes, R. H., Emmons, L. K., Orlando, J. J., Barth, M. C., Tyndall, G. S., Hall, S. R., Ullmann, K., St. Clair, J. M., Blake, D. R., Wisthaler, A., and Bui, T. P. V.: Comprehensive isoprene and terpene gas-phase chemistry improves simulated surface ozone in the southeastern US, Atmospheric Chemistry and Physics, 20, 3739–3776, https://doi.org/10.5194/acp-20-3739-2020, publisher: Copernicus GmbH, 2020.

Schwartz, S. E.: Mass-Transport Considerations Pertinent to Aqueous Phase Reactions of Gases in Liquid-Water Clouds, in: Chemistry of Multiphase Atmospheric Systems, edited by Jaeschke, W., NATO ASI Series, pp. 415–471, Springer, Berlin, Heidelberg, https://doi.org/10.1007/978-3-642-70627-1_16, 1986.

Seinfeld, J. H. and Pandis, S. N.: Atmospheric Chemistry and Physics: From Air Pollution to Climate Change, Wiley, 3 edn., 2016.

Sorooshian, A., Varutbangkul, V., Brechtel, F. J., Ervens, B., Feingold, G., Bahreini, R., Murphy, S. M., Holloway, J. S., Atlas, E. L., Buzorius, G., Jonsson, H., Flagan, R. C., and Seinfeld, J. H.: Oxalic acid in clear and cloudy atmospheres: Analysis of data from International Consortium for Atmospheric Research on Transport and Transformation 2004, Journal of Geophysical Research: Atmospheres, 111, https://doi.org/10.1029/2005JD006880, 2006.

Sorooshian, A., Ng, N. L., Chan, A. W. H., Feingold, G., Flagan, R. C., and Seinfeld, J. H.: Particulate organic acids and overall water-soluble aerosol composition measurements from the 2006 Gulf of Mexico Atmospheric Composition and Climate Study (GoMACCS), Journal of Geophysical Research: Atmospheres, 112, https://doi.org/10.1029/2007JD008537, 2007.

Sorooshian, A., Wang, Z., Coggon, M. M., Jonsson, H. H., and Ervens, B.: Observations of Sharp Oxalate Reductions in Stratocumulus Clouds at Variable Altitudes: Organic Acid and Metal Measurements During the 2011 E-PEACE Campaign, Environmental Science & Technology, 47, 7747–7756, https://doi.org/10.1021/es4012383, 2013.

Souza, S. R., Vasconcellos, P. C., and Carvalho, L. R. F.: Low molecular weight carboxylic acids in an urban atmosphere: Winter measurements in São Paulo City, Brazil, Atmospheric Environment, 33, 2563–2574, https://doi.org/10.1016/S1352-2310(98)00383-5, 1999.

Stein, A. F., Draxler, R. R., Rolph, G. D., Stunder, B. J. B., Cohen, M. D., and Ngan, F.: NOAA's HYSPLIT Atmospheric Transport and Dispersion Modeling System, Bulletin of the American Meteorological Society, 96, 2059–2077, https://doi.org/10.1175/BAMS-D-14-00110.1, 2015.

Stone, B. J., Gronlund, C. J., Mallen, E., Hondula, D., O'Neill, M. S., Rajput, M., Grijalva, S., Lanza, K., Harlan, S., Larsen, L., Augenbroe, G., Krayenhoff, E. S., Broadbent, A., and Georgescu, M.: How Blackouts during Heat Waves Amplify Mortality and Morbidity Risk, Environmental Science & Technology, 57, 8245–8255, https://doi.org/10.1021/acs.est.2c09588, publisher: American Chemical Society, 2023.

Tan, Y., Carlton, A. G., Seitzinger, S. P., and Turpin, B. J.: SOA from methylglyoxal in clouds and wet aerosols: Measurement and prediction of key products, Atmospheric Environment, 44, 5218–5226, https://doi.org/10.1016/j.atmosenv.2010.08.045, 2010.

Tao, Y. and Murphy, J. G.: Evidence for the Importance of Semivolatile Organic Ammonium Salts in Ambient Particulate Matter, Environmental Science & Technology, 53, 108–116, https://doi.org/10.1021/acs.est.8b03800, publisher: American Chemical Society, 2019.

Tian, Y., LaFarr, M., Yun, J., Civerolo, K., Hao, W., Zalewsky, E., and Zhou, L.: Analyzing Meteorological and Chemical Conditions for Two High Ozone Events Over the New York City and Long Island Region, in: IGARSS 2020 - 2020 IEEE International Geoscience and Remote Sensing Symposium, pp. 5537–5540, https://doi.org/10.1109/IGARSS39084.2020.9324470, iSSN: 2153-7003, 2020.

Tilgner, A. and Herrmann, H.: Radical-driven carbonyl-to-acid conversion and acid degradation in tropospheric aqueous systems studied by CAPRAM, Atmospheric Environment, 44, 5415–5422, https://doi.org/10.1016/j.atmosenv.2010.07.050, 2010.

Tilgner, A. and Herrmann, H.: Tropospheric Aqueous-Phase OH Oxidation Chemistry: Current Understanding, Uptake of Highly Oxidized Organics and Its Effects, in: Multiphase Environmental Chemistry in the Atmosphere, vol. 1299 of *ACS Symposium Series*, pp. 49–85, American Chemical Society, https://doi.org/10.1021/bk-2018-1299.ch004, section: 4, 2018.

Tran, T., Kumar, N., and Knipping, E.: Investigating sensitivity of ozone to emission reductions in the New York City (NYC) metropolitan and downwind areas, Atmospheric Environment, 301, 119 675, https://doi.org/10.1016/j.atmosenv.2023.119675, 2023.

Travis, K. R., Jacob, D. J., Fisher, J. A., Kim, P. S., Marais, E. A., Zhu, L., Yu, K., Miller, C. C., Yantosca, R. M., Sulprizio, M. P., Thompson, A. M., Wennberg, P. O., Crounse, J. D., St. Clair, J. M., Cohen, R. C., Laughner, J. L., Dibb, J. E., Hall, S. R., Ullmann, K., Wolfe, G. M., Pollack, I. B., Peischl, J., Neuman, J. A., and Zhou, X.: Why do models overestimate surface ozone in the Southeast United States?, Atmospheric Chemistry and Physics, 16, 13 561–13 577, https://doi.org/10.5194/acp-16-13561-2016, publisher: Copernicus GmbH, 2016.

Wang, M., Perroux, H., Fleuret, J., Bianco, A., Bouvier, L., Colomb, A., Borbon, A., and Deguillaume, L.: Anthropogenic and biogenic hydrophobic VOCs detected in clouds at the puy de Dôme station using Stir Bar Sorptive Extraction: Deviation from the Henry's law prediction, Atmospheric Research, 237, 104 844, https://doi.org/10.1016/j.atmosres.2020.104844, 2020.

Wang, Z., Chen, X., Liang, Y., and Shi, Q.: Molecular characterization of carbonyl compounds in atmospheric fine particulate matters (PM2.5) in Beijing by derivatization with Girard's reagent T combined with positive-ion ESI Orbitrap MS, Atmospheric Research, 273, 106 176, https://doi.org/10.1016/j.atmosres.2022.106176, 2022.

Warneck, P.: Multi-Phase Chemistry of C2 and C3 Organic Compounds in the Marine Atmosphere, Journal of Atmospheric Chemistry, 51, 119–159, https://doi.org/10.1007/s10874-005-5984-7, 2005.

Wilcox, R. R.: Introduction to robust estimation and hypothesis testing, Statistical modeling and decision science, Academic Press, Amsterdam ; Boston, 3rd ed edn., 2012.

Winiwarter, W., Fierlinger, H., Puxbaum, H., Facchini, M. C., Arends, B. G., Fuzzi, S., Schell, D., Kaminski, U., Pahl, S., Schneider, T., Berner, A., Solly, I., and Kruisz, C.: Henry's law and the behavior of weak acids and bases in fog and cloud, Journal of Atmospheric Chemistry, 19, 173–188, https://doi.org/10.1007/BF00696588, 1994.

Wolfe, G. M., Marvin, M. R., Roberts, S. J., Travis, K. R., and Liao, J.: The Framework for 0-D Atmospheric Modeling (F0AM) v3.1, Geoscientific Model Development, 9, 3309–3319, https://doi.org/10.5194/gmd-9-3309-2016, publisher: Copernicus GmbH, 2016.

Yao, X., Fang, M., Chan, C. K., Ho, K. F., and Lee, S. C.: Characterization of dicarboxylic acids in PM2.5 in Hong Kong, Atmospheric Environment, 38, 963–970, https://doi.org/10.1016/j.atmosenv.2003.10.048, 2004.

Yuan, B., Veres, P. R., Warneke, C., Roberts, J. M., Gilman, J. B., Koss, A., Edwards, P. M., Graus, M., Kuster, W. C., Li, S.-M., Wild, R. J., Brown, S. S., Dubé, W. P., Lerner, B. M., Williams, E. J., Johnson, J. E., Quinn, P. K., Bates, T. S., Lefer, B., Hayes, P. L., Jimenez, J. L., Weber, R. J., Zamora, R., Ervens, B., Millet, D. B., Rappenglück, B., and de Gouw, J. A.: Investigation of secondary formation of formic acid: urban environment vs. oil and gas producing region, Atmospheric Chemistry and Physics, 15, 1975–1993, https://doi.org/10.5194/acp-15-1975-2015, publisher: Copernicus GmbH, 2015.

Zhang, H., Kupiainen-Määttä, O., Zhang, X., Molinero, V., Zhang, Y., and Li, Z.: The enhancement mechanism of glycolic acid on the formation of atmospheric sulfuric acid–ammonia molecular clusters, The Journal of Chemical Physics, 146, 184 308, https://doi.org/10.1063/1.4982929, publisher: American Institute of Physics, 2017.

Zhang, R., Suh, I., Zhao, J., Zhang, D., Fortner, E. C., Tie, X., Molina, L. T., and Molina, M. J.: Atmospheric New Particle Formation Enhanced by Organic Acids, Science, 304, 1487–1490, https://doi.org/10.1126/science.1095139, publisher: American Association for the Advancement of Science, 2004.

Zhu, Y., Tilgner, A., Hoffmann, E. H., Herrmann, H., Kawamura, K., Yang, L., Xue, L., and Wang, W.: Multiphase MCM/CAPRAMmodeling of formation and processing of secondary aerosol constituents observed at the Mt. Tai summer campaign 2014, Atmospheric Chemistry and Physics Discussions, pp. 1–39, https://doi.org/https://doi.org/10.5194/acp-2019-982, publisher: Copernicus GmbH, 2019.

Zuo, Y. and Hoigne, J.: Formation of hydrogen peroxide and depletion of oxalic acid in atmospheric water by photolysis of iron(III)-oxalato complexes, Environmental Science & Technology, 26, 1014–1022, https://doi.org/10.1021/es00029a022, 1992.